A LIFTING SURFACE THEORY

FOR

WINGS AT HIGH ANGLES OF ATTACK

EXTENDING THROUGH MULTIPLE JETS

E. Cumberbatch

VEHICLE RESEARCH CORPORATION

PASADENA, CALIFORNIA

A LIFTING SURFACE THEORY

FOR

WINGS AT HIGH ANGLES OF ATTACK

EXTENDING THROUGH MULTIPLE JETS

E.   Cumberbatch

Conducted for

THE OFFICE OF NAVAL RESEARCH

under

Contract No.   Nonr 2388(00)

VRC Report No. 9

26 July 1963

VEHICLE RESEARCH CORPORATION
161 East California Boulevard
Pasadena, California

SYcamore 5-0491

FOREWORD

This report consists of the first and second parts of the three part analytical portion of the High Angle of Attack Theory (third phase) of VRC's program of developing methods for assessing the non-uniform flow fields of wing-propeller slipstream aerodynamics. The overall program, consisting of four (4) phases as described in Ref. 1, was undertaken to generalize and extend the basic Rethorst Lifting Surface Theory (Ref. 2).

The first phase (Ref. 3) was comprised of an application of the basic Single Jet (Propeller Slipstream) Theory (Ref. 2) to delineate optimum finite wing planforms. In the second phase (Ref. 1) the Single Jet Theory was generalized and extended into a Multiple Jet Theory. The generalizations and refinements of the second phase have established a solid foundation for the third phase (present report).

The three parts of the third phase effort are comprised of:

1. Wings located at various heights in the jet

2. Highly cambered wings as used in deflected slipstream V/STOL arrangements

3. Tilt wing configurations where the jet is at an angle to the free stream flow

The present report contains the basic theorectical development of the first two parts enumerated above. This portion of the third phase effort has greatly extended the applicability of the analysis by encompassing deflected slipstream V/STOL arrangements currently under development.

SUMMARY

A lifting surface theory has been developed for wings located
at arbitrary heights and high angles of attack (up to the inception of
flow separation) in a stream containing an arbitrary number of multiple
jets (propeller slipstreams). This theory extends and generalizes the
formulation of T. Y. Wu and Richard B. Talmadge (VRC Report No. 8)
which was based on the original Rethorst Lifting Surface Solution.

The present theory was developed by first analyzing the simpler
single jet case and then extending the analysis to encompass multiple
jets. Thus, the analysis is systematically presented in the following
order:

1. Wing at an Arbitrary Height in a Single Jet - a method
similar to that employed in VRC Report No. 8 for the wing located along
the axis of the jet was used to extend the solution to a wing located at
any height in the jet.

2. Wing at a High Angle of Attack in a Single Jet - the lifting
surface method of Weissinger was applied to chordwise wing sections each
of which is treated in accordance with its height in the jet as determined
in the previous step.

3. Wing at Arbitrary Height and High Angle of Attack Extending
through Multiple Jets - the above single jet analyses were extended to the
case of a wing immersed in a stream containing an arbitrary number of jets.
The jets were located symmetrically in the spanwise direction.

The above generalized theory encompasses a broad spectrum of
V/STOL aircraft. The prediction of wing-slipstream interactions afforded
by the present analysis permits optimization of such V/STOL aircraft.

TABLE OF CONTENTS

I. INTRODUCTION

This paper provides an extension to the work of T. Y. Wu and Richard B. Talmadge,[1] who considered the problem of a wing at a small angle of attack placed along the center line of a number of jets. Previous attacks on this problem are listed and discussed by Wu. The effect of varying the height of a wing in jet slipstreams has not been considered previously to the knowledge of the author. A solution is obtained in the present paper for a wing at an arbitrary position and angle of attack, consistent with the assumption of non-separated flow, in a stream containing a single or a number of circular jets symmetrically placed along the wing.

The problem of a wing at an arbitrary height in a single jet is treated in Section II by similar methods to those used by Wu for the wing at the center of the jet. In this latter case the wing is represented by a bound vortex line centered along the quarter-chord line of the wing, plus a trailing vortex system, the boundary condition on the wing being satisfied along the three-quarter-chord line. The solution for a wing at a moderate angle of attack in a single jet is presented in Section III using the Weissinger method in which the wing is divided chordwise into a number of sections; the solution for each section of the wing is then given by the relevant solution of Section II corresponding to the height of the section. In this way a bound vortex line is placed at the quarter-chord point of each section and the boundary conditions necessary to determine the vortex strength are satisfied at the three-quarter-chord point of each section. The problem of a wing at moderate inclinations extending through a number of jets is attacked in Section IV by extensions

from the single jet case using the techniques developed by Wu.

The solutions described above are derived from a superposition of infinitesimal vortex elements. The solution for each vortex element is found by splitting the element into a two- and a three-dimensional part. The image system due to the presence of a circular jet in the main stream is easily determined for the two-dimensional part. A similar image system for the three-dimensional part is assumed plus a remainder term, which is then determined by the boundary conditions on the jet boundary. A feature of this approach is that the complicated part of the analysis is contained in the remainder term, which for the examples computed by Wu so far has contributed only a small amount to the total lift. No justification for neglecting this part has yet been found however and it remains necessary to include it in the present treatment.

Certain simplifying assumptions are made as follows. The flow is assumed incompressible and inviscid, in which case a velocity potential exists for the flow inside and outside the jets, though this potential need not be continuous across the jet boundary. The jet boundary may thus be regarded as a circular vortex sheet. The slipstream jets are assumed to be circular in cross section having a velocity V_j parallel to the main stream of velocity V_o. The coefficient

$$\mu = V_o / V_j \tag{1}$$

is formed. The jets are assumed to be only slightly distorted by the wing so that the boundary conditions on the jet boundary may be applied on the undisturbed circular boundary. These boundary conditions are the kinematic

condition that the flow just interior and exterior to the jet boundary must be parallel, and the dynamic condition that the pressure must be continuous across the jet boundary. Dealing for the moment with a single jet of unit radius whose axis is taken along the x-axis, the velocities outside and inside the jet are taken to be

$$\vec{v}_o = V_o \vec{i} + \nabla \varphi_o , \qquad \vec{v}_j = V_j \vec{i} + \nabla \varphi_j \qquad (2)$$

where φ_o and φ_j denote the perturbation velocity potentials outside and inside the jet, respectively. The boundary conditions on the jet boundary may then be expressed as

$$\frac{\partial \varphi_o}{\partial q} = \mu \frac{\partial \varphi_j}{\partial q} \qquad \text{on} \quad q = \sqrt{y^2 + z^2} = 1 \qquad (3)$$

and

$$\frac{\partial \varphi_j}{\partial x} = \mu \frac{\partial \varphi_o}{\partial x} \qquad \text{on} \quad q = 1 \qquad (4)$$

where in the latter a linearized Bernoulli equation has been used. Eq. 4 may be integrated from $x = -\infty$ to give

$$\varphi_j = \mu \varphi_o \qquad \text{on} \quad r = 1 \qquad (5)$$

where it has been assumed that the potentials vanish at $x = -\infty$.

II. SOLUTION FOR A WING AT AN ARBITRARY HEIGHT

IN A SINGLE JET

A. FORMULATION

The analysis presented in this section is concerned with a wing represented by a bound vortex lying along the line given by $x = 0$ and $z = -h$ from $y = -b_1$ to $y = b_2$, and its trailing vortex system. A superposition of these solutions along the chord will then be used in Section 3 to represent a wing at a moderate angle of attack in the jet. The jet is located with its axis along the x-axis and is taken to have unit radius (see Fig. 1). A point in the y-z plane is expressed as

$$r = y + iz = qe^{i\theta} \tag{6}$$

and a point on the wing, $y = \eta$, is given by

$$r_o = \eta - ih = se^{-i\alpha} \quad \text{for} \quad -b_1 \leq \eta \leq b_2 \tag{7}$$

The solution for an infinitesimal element of bound vorticity has been given by von Karman (a derivation is given by Wu). The result for a bound vortex element of strength $\Gamma(\eta)\delta\eta$, located along the wing $x = 0$, $z = -h$, for $\eta < y < \eta + \delta\eta$ is

$$\delta\varphi = \delta\varphi_2 + \delta\varphi_3 \tag{8}$$

where

$$\delta\varphi_2 = \frac{1}{4\pi}\Gamma(\eta)\delta\eta\, F_1(y-\eta,z+h) = \frac{1}{4\pi}\Gamma(\eta)\delta\eta\, \frac{z+h}{(y-\eta)^2+(z+h)^2}$$

$$\delta\varphi_3 = \frac{1}{4\pi}\Gamma(\eta)\delta\eta\, F_2(x,y-\eta,z+h)$$

$$= \frac{1}{4\pi}\Gamma(\eta)\delta\eta\, \frac{z+h}{(y-\eta)^2+(z+h)^2}\, \frac{x}{[x^2+(y-\eta)^2+(z+h)^2]^{1/2}}$$

The velocity potential in 8 has been split into two parts $\delta\varphi_2$ and $\delta\varphi_3$, representing the two- and three-dimensional parts of the solution. The effect of the jet on the solution 8 for the vortex element will be derived in parts B, C, and D of this section, for the two- and three-dimensional parts of the solution, respectively. The solution for the whole wing will be given in part E by integrating the vorticity distribution $\Gamma(\eta)$ from $y = -b_1$ to $y = b_2$.

B. IMAGE SYSTEM FOR THE TWO-DIMENSIONAL PART OF THE SOLUTION

The effect of the jet, represented by the boundary conditions 3 and 5, on the two-dimensional part $\delta\varphi_2$ of the vortex element 8 is determined in this section. A simple method to do this is to express $\delta\varphi_2$ as the difference of logarithmic terms representing simple line vortices situated very close together. The effect of the jet is found for each line vortex by choice of a suitable image system to satisfy the boundary conditions 3 and 5 on $r = 1$, the boundary of the jet. Two separate cases of the vortex element lying outside or inside the jet are to be considered, that is $s^2 = \eta^2 + h^2 > 1$ or $s^2 < 1$, respectively. The two-dimensional part of the solution is then

- 5 -

(i) $s > 1$, i. e. for vortex element outside jet

$$\delta\varphi_2 = \begin{cases} \dfrac{1}{4\pi}\,\Gamma(\eta)\delta\eta\left\{F_1(y-\eta,z+h) + \dfrac{\epsilon_1}{s^4}\left[(\eta^2-h^2)F_1(y-\dfrac{\eta}{s^2},z+\dfrac{h}{s^2})\right.\right. \\ \qquad\qquad \left.\left. + 2\eta h F_3(y-\dfrac{\eta}{s^2},z+\dfrac{h}{s^2})\right]\right\} \qquad\qquad \text{for } q > 1 \\[2em] \dfrac{1}{4\pi}\,\Gamma(\eta)\delta\eta\left\{(1-\epsilon_2)F_1(y-\eta,z+h) - \mu\epsilon_1 F_1(\eta,h)\right\} \quad \text{for } q < 1 \end{cases}$$

(9)

(ii) $s < 1$, i. e. for vortex element inside jet

$$\delta\varphi_2 = \begin{cases} \dfrac{1}{4\pi}\,\Gamma(\eta)d\eta\left\{(1-\epsilon_2)F_1(y-\eta,z+h)\right\} \qquad\qquad \text{for } q > 1 \\[2em] \dfrac{1}{4\pi}\,\Gamma(\eta)d\eta\left\{F_1(y-\eta,z+h) - \dfrac{\epsilon_1}{s^4}\left[(\eta^2-h^2)F_1(y-\dfrac{\eta}{s^2},z+\dfrac{h}{s^2})\right.\right. \\ \qquad\qquad \left.\left. + 2\eta h F_3(y-\dfrac{\eta}{s^2},z+\dfrac{h}{s^2})\right] - \epsilon_1 F_1(\eta,h)\right\} \quad \text{for } q < 1 \end{cases}$$

(10)

where

$$\epsilon_1 = \frac{1-\mu^2}{1+\mu^2}, \qquad \epsilon_2 = \frac{(1-\mu)^2}{1+\mu^2}.$$

and

(11)

$$F_3(y,z) = \frac{y}{y^2+z^2}$$

It may be noted that the terms $F_1(\eta,h)$ in the solutions above are constant terms in the potential and hence may be omitted; their inclusion resulted from using the boundary condition 5 on the potential rather than 4 and its derivative.

The two-dimensional part of the solution corresponding to a lifting vortex line of given circulation distribution $\Gamma(y)$ extending from $y = -b_1$ to

$y = \dot{b}_2$, may now be obtained from 9 and 10 by linear superposition. Hence one obtains

$$4\pi\,\varphi_2 = \int_{-b_1}^{b_2} \Gamma(\eta)F_1(y-\eta,\,z+h)d\eta - \epsilon_2\int_{-h'}^{h'}\Gamma(\eta)F_1(y-\eta,\,z+h)d\eta$$

$$+ \epsilon_1\left\{\int_{-b_1}^{-h'} + \int_{h'}^{b_2}\right\}\frac{\Gamma(\eta)}{s^4}\left[(\eta^2-h^2)F_1(y-\frac{\eta}{s^2},\,z+\frac{h}{s^2})\right.$$

$$\left. + 2\eta h F_3(y-\frac{\eta}{s^2},\,z+\frac{h}{s^2})\right]d\eta \qquad \text{for } q > 1, \quad (12)$$

$$4\pi\varphi_2 = \int_{-b_1}^{b_2} \Gamma(\eta)F_1(y-\eta,\,z+h)d\eta - \epsilon_2\left\{\int_{-b_1}^{-h'} + \int_{h'}^{b_2}\right\}\Gamma(\eta)F_1(y-\eta,\,z+h)d\eta$$

$$- \epsilon_1\int_{-h'}^{h'}\frac{\Gamma(\eta)}{s^4}\left[(\eta^2-h^2)F_1(y-\frac{\eta}{s^2},\,z+\frac{h}{s^2})\right.$$

$$\left. + 2\eta h F_3(y-\frac{\eta}{s^2},\,z+\frac{h}{s^2})\right]d\eta \qquad \text{for } q < 1, \quad (13)$$

where

$$h' = \sqrt{1 - h^2}.$$

C. THE THREE-DIMENSIONAL PART OF THE SOLUTION FOR THE VORTEX ELEMENT LOCATED OUTSIDE THE JET

The effect of the jet on the three-dimensional part $\delta\varphi_3$ of the vortex element 8 is determined. The vortex element is taken to be located outside the jet, i.e. $s > 1$; the case of $s < 1$ is dealt with in Section II-D. The image method used for the two-dimensional part cannot be used here as the problem is considerably more complicated. The technique--introduced by Wu--of using a similar image system as the two-dimensional one, plus a remainder term

which is then to be determined by the boundary conditions 3 and 5, will be used. Using 8 and 9, the proposed form for the vortex element is

$$\delta\varphi_3 = \frac{1}{4\pi}\,\Gamma(\eta)\,\delta\eta\,\left\{\varphi_o' + F_2(x, y-\eta, z+h)\right.$$

$$\left.+\frac{\epsilon_1}{s^4}\left[(\eta^2-h^2)F_2(x, y-\frac{\eta}{s^2}, z+\frac{h}{s^2}) + 2\eta h F_4(x, y-\frac{\eta}{s^2}, z+\frac{h}{s^2})\right]\right\}$$

$$\text{for } q > 1, \quad (14)$$

$$\delta\varphi_3 = \frac{1}{4\pi}\,\Gamma(\eta)\,\delta\eta\,\left\{\varphi_j' + (1-\epsilon_2)F_2(x, y-\eta, z+h)\right\} \qquad \text{for } q < 1, \quad (15)$$

where

$$F_4(x, y, z) = \frac{y}{y^2+z^2}\,\frac{x}{(x^2+y^2+z^2)^{1/2}} \tag{16}$$

and F_2 has been defined in 8. Here φ_o' and φ_j' are the remainder terms left in the potential after subtracting the F-functions representing a convenient image system: φ_o', φ_j' satisfy Laplace's equation outside and inside the jet, respectively.

Application of 3 and 5 yields the following boundary conditions on φ_o' and φ_j'

$$(\varphi_j' - \mu\varphi_o')_{q=1} = \epsilon_1\mu\left\{-F_2(x, y-\eta, z+h)\right.$$

$$\left.+\frac{1}{s^4}\left[(\eta^2-h^2)F_2(x, y-\frac{\eta}{s^2}, z+\frac{h}{s^2}) + 2\eta h F_4(x, y-\frac{\eta}{s^2}, z+\frac{h}{s^2})\right]\right\} \tag{17}$$

$$\left(\frac{\partial\varphi_o'}{\partial q} - \mu\frac{\partial\varphi_j'}{\partial q}\right)_{q=1} = -\epsilon_1\frac{\partial}{\partial q}\left\{F_2(x, y-\eta, z+h)\right.$$

$$\left.+\frac{1}{s^4}\left[(\eta^2-h^2)F_2(x, y-\frac{\eta}{s^2}, z+\frac{h}{s^2}) + 2\eta h F_4(x, y-\frac{\eta}{s^2}, z+\frac{h}{s^2})\right]\right\} \tag{18}$$

where

$$y = q \cos \theta, \qquad z = q \sin \theta \tag{19}$$

and $q = 1$ must be substituted on the right-hand side. From 17 and 18, or from subsequent forms of these expressions, it may be shown that φ_0' and φ_j' and their derivatives are well-behaved near both $x = 0$ and $x = \infty$. Also φ_0' and φ_j' are odd functions in the x-variable, which leads to the following representations of these harmonic functions

$$\varphi_0' = \frac{2}{\pi} \sum_{m=0}^{\infty} \left\{ \sin m\theta \int_0^{\infty} S_m^{(o)}(k, s) K_m(kq) \sin kx \, dk \right.$$

$$\left. + \cos m\theta \int_0^{\infty} C_m^{(o)}(k, s) K_m(kq) \sin kx \, dk \right\} \qquad \text{for } q > 1, \tag{20}$$

$$\varphi_j' = \frac{2}{\pi} \sum_{m=0}^{\infty} \left\{ \sin m\theta \int_0^{\infty} S_m^{(j)}(k, s) I_m(k, q) \sin kx \, dk \right.$$

$$\left. + \cos m\theta \int_0^{\infty} C_m^{(j)}(k, s) I_m(kq) \sin kx \, dk \right\} \qquad \text{for } q < 1 . \tag{21}$$

The functions I_m and K_m are the modified Bessel functions of the first and second kind, respectively, as defined in Ref. 2. K_m is used in the solution outside the jet, and I_m is used inside the jet, to ensure that φ_0' and φ_j' will be regular at $q = \infty$ and $q = 0$, respectively. The super-indices (o) and (j) chacterize the region of definition of the functions S and C, i.e. outside or inside the jet. The functions S and C are to be determined from the boundary conditions 17 and 18.

The expressions on the right-hand sides of 17 and 18 are now expanded into similar series and integral forms used in representing φ_0' and

φ'_j above. The integral representations of the F-functions, demonstrated by

$$F_2(x, y, z) = \frac{z}{y^2+z^2} \frac{x}{(x^2+y^2+z^2)^{1/2}} = z \int_0^x (\xi^2+y^2+z^2)^{-3/2} d\xi, \quad (22)$$

are used in 17 and 18 to give the following relations

$$(\varphi'_j - \mu\varphi'_o)_{q=1} = \mu\epsilon_1 \left\{ (\sin\theta + h) \int_x^{xs} [\xi^2 + s^2 + 1 - 2s \cos(\theta+\alpha)]^{-3/2} d\xi \right.$$

$$\left. - \frac{1}{s} hx [x^2 s^2 + s^2 + 1 - 2s \cos(\theta+\alpha)]^{-1/2} \right\} \quad (23)$$

$$\left(\frac{\partial\varphi'_o}{\partial q} - \mu \frac{\partial\varphi'_j}{\partial q} \right)_{q=1} = \epsilon_1 \left\{ x(\sin\theta+h)[x^2 + s^2 + 1 - 2s \cos(\theta+\alpha)]^{-3/2} \right.$$

$$- hx[s-\cos(\theta+\alpha)][x^2 s^2 + s^2 + 1 - 2s \cos(\theta+\alpha)]^{-3/2}$$

$$\left. - \frac{\partial}{\partial q} \int_x^{xs} (q \sin\theta + hq^2)[\xi^2 + q^2 s^2 + 1 - 2sq \cos(\theta+\alpha)]^{-3/2} d\xi \right\}$$

$$(24)$$

in which $q = 1$ has to be substituted on the right-hand side.

The following expansions in terms of Bessel functions are used in 23 and 24. These relations are given in Watson[4] or may be deduced from relations there. They are

$$x(x^2 + s^2 + 1 - 2s \cos\theta)^{-3/2} = \frac{2}{\pi} \int_0^\infty k \sin kx \, K_o(k\sqrt{s^2+1-2s\cos\theta}) \, dk \quad (25)$$

$$\int_x^{sx} (\xi^2 + s^2 + 1 - 2s \cos\theta)^{-3/2} d\xi = \frac{2}{\pi} \int_0^\infty \frac{1}{k} \sin kx \, dk \int_{\frac{1}{s}k}^k t K_o(t\sqrt{s^2+1-2s\cos\theta}) \, dt$$

$$(26)$$

- 10 -

$$(\mu^2 - \nu^2) \int^y x I_n(\mu x) K_n(\nu x) dx = y \left\{ \mu K_n(\nu y) I_{n-1}(\mu y) + \nu K_{n-1}(\nu y) I_n(\mu y) \right\} \tag{27}$$

$$K_o(t\sqrt{1 + s^2 - 2s \cos \theta})$$

$$= K_o(ts) I_o(t) + 2 \sum_{m=1}^{\infty} K_m(ts) I_m(t) \cos m\theta \qquad \text{for } s > 1$$

$$\tag{28}$$

$$= K_o(t) I_o(ts) + 2 \sum_{m=1}^{\infty} K_m(t) I_m(ts) \cos m\theta \qquad \text{for } s < 1$$

$$\sin \theta K_o(t\sqrt{s^2 + 1 - 2s \cos \theta})$$

$$= \sum_{n=1}^{\infty} \left[I_{n-1}(t) K_{n-1}(st) - I_{n+1}(t) K_{n+1}(st) \right] \sin n\theta \qquad \text{for } s > 1$$

$$\tag{29}$$

$$= \sum_{n=1}^{\infty} \left[I_{n-1}(st) K_{n-1}(t) - I_{n+1}(st) K_{n+1}(t) \right] \sin n\theta \qquad \text{for } s < 1$$

Using such identities as above, Eqs. 23 and 24 may now be written in the form

$$(\varphi_j' - \mu \varphi_o')_{q=1}$$

$$= \frac{2\mu\epsilon_1}{\pi} \int_0^{\infty} \sin kx \left\{ \sin \alpha \left[\frac{1}{s^2} K_o(k) I_1(\frac{k}{s}) - K_1(ks) I_o(k) \right] \right.$$

$$+ 2 \sum_{m=1}^{\infty} \left(\frac{m}{ks} \left[K_m(k) I_m(\frac{k}{s}) - K_m(ks) I_m(k) \right] \cos \alpha \sin m(\alpha + \theta) \right.$$

$$\left. + \left[K_m'(sk) I_m(k) + \frac{1}{s^2} K_m(k) I_m'(\frac{k}{s}) \right] \sin \alpha \cos m(\alpha + \theta) \right) \right\} dk$$

$$\tag{30}$$

- 11 -

$$\left(\frac{\partial \varphi_o'}{\partial q} - \mu \frac{\partial \varphi_j'}{\partial q} \right)_{q=1}$$

$$= \frac{2\epsilon_1}{\pi} \int_0^\infty \sin kx \left\{ -k \sin \alpha \left[K_1(sk)I_1(s) - \frac{1}{s^2} K_1(k)\dot{I}_1(\frac{k}{s}) \right] \right.$$

$$+ 2 \sum_{m=1}^\infty \left(k \left[K_m'(ks)I_m'(k) - \frac{1}{s^2} K_m'(k)I_m'(\frac{k}{s}) \right] \sin \alpha \cos m(\alpha+\theta) \right.$$

$$\left. \left. - \frac{m}{s} \left[K_m(ks)I_m'(k) + K_m'(k)I_m(\frac{k}{s}) \right] \cos \alpha \sin m(\alpha+\theta) \right) \right\} dk$$

$$(31)$$

where K_m' and I_m' denote the derivative of K_m and I_m.

The boundary conditions 3 and 5, represented by 30 and 31, are now in a form suitable for comparison with similar expressions obtained from the expansions 20 and 21 assumed for the solution. The S_m and C_m coefficients in 20 and 21 may then be determined. Hence

$$S_m^{(o)}(k, s) = 2\epsilon_1 \left\{ \frac{m}{ks} \left[-I_m(\frac{k}{s}) + \frac{2kI_m I_m' K_m(ks)}{1 - \epsilon_1 k(I_m K_m' + K_m I_m')} \right] \cos \alpha \cos m\alpha \right.$$

$$\left. + \left[\frac{1}{s^2} I_m'(\frac{k}{s}) + \frac{2kI_m I_m' K_m'(ks)}{1 - \epsilon_1 k(I_m K_m' + K_m I_m')} \right] \sin \alpha \sin m\alpha \right\} \quad (32a)$$

$$S_m^{(j)}(k, s) = 2\epsilon_1(1-\epsilon_2)k \frac{I_m K_m' + K_m I_m'}{1 - \epsilon_1 k(I_m K_m' + K_m I_m')} \left\{ \frac{m}{ks} K_m(ks)\cos \alpha \cos m\alpha \right.$$

$$\left. + K_m'(ks) \sin \alpha \sin m\alpha \right\} \quad (32b)$$

$$C_m^{(o)}(k,s) = 2\epsilon_1 \left\{ \frac{m}{ks} \left[-I_m(\frac{k}{s}) + \frac{2kI_m I_m' K_m(ks)}{1-\epsilon_1 k(I_m K_m' + K_m I_m')} \right] \cos \alpha \sin m\alpha \right.$$

$$\left. -\left[\frac{1}{s^2} I_m'(\frac{k}{s}) + \frac{2kI_m I_m' K_m'(ks)}{1-\epsilon_1 k(I_m K_m' + K_m I_m')} \right] \sin \alpha \cos m\alpha \right\}$$

$$(32c)$$

$$C_m^{(j)}(k,s) = 2\epsilon_1(1-\epsilon_2)k \frac{I_m K_m' + K_m I_m'}{1-\epsilon_2 k(I_m K_m' + K_m I_m')} \left\{ \frac{m}{ks} K_m(ks)\cos \alpha \sin m\alpha \right.$$

$$\left. - K_m'(ks)\sin \alpha \cos m\alpha \right\}$$

$$(32d)$$

Here, the argument for the Bessel functions of argument k has been omitted for brevity. Eqs. 32 provide the coefficients necessary to evaluate φ_o' and φ_j' from 20 and 21 and hence the three-dimensional part of the solution for the vortex element lying outside the jet is established.

D. THE THREE-DIMENSIONAL PART OF THE SOLUTION FOR THE VORTEX ELEMENT LOCATED INSIDE THE JET

In this section a solution is developed for the three-dimensional vortex element given by 8 in the presence of a circular jet, for the case in which the element is located inside the jet, i. e. $s < 1$. Similar techniques to II-C are used. The vortex element is represented by

$$\delta\varphi_3 = \frac{1}{4\pi} \Gamma(\eta)\delta\eta \left\{ \varphi_o' + (1-\epsilon_2)F_2(x,y-\eta,z+h) \right\} \qquad \text{for } q > 1 \qquad (33)$$

$$\delta\varphi_3 = \frac{1}{4\pi} \Gamma(\eta)\delta\eta \left\{ \varphi_j' + F_2(x,y-\eta,z+h) - \frac{\epsilon_1}{s^4} \left[(\eta^2-h^2)F_2(x,y-\frac{\eta}{s^2},z+\frac{h}{s^2}) \right. \right.$$

$$\left. \left. + 2\eta h F_4(x,y-\frac{\eta}{s^2},z+\frac{h}{s^2}) \right] \right\} \qquad \text{for } q < 1 \qquad (34)$$

Here φ_o' and φ_j' are the remainder terms left in the potential after subtracting the F-functions representing a similar image system to the two-dimensional one (see 10). The harmonic functions φ_o', φ_j' are odd in x, and regular near both $x = 0$ and $x = \infty$; they may therefore be represented by the expansions

$$\varphi_o' = \frac{2}{\pi} \sum_{m=0}^{\infty} \left\{ \sin m\theta \int_0^{\infty} T_m^{(o)}(k,s) K_m(kq) \sin kx \, dk \right.$$

$$\left. + \cos m\theta \int_0^{\infty} D_m^{(o)}(k,s) K_m(kq) \sin kx \, dk \right\} \quad \text{for } q > 1 \quad (35)$$

$$\varphi_j' = \frac{2}{\pi} \sum_{m=0}^{\infty} \left\{ \sin m\theta \int_0^{\infty} T_m^{(j)}(k,s) I_m(kq) \sin kx \, dk \right.$$

$$\left. + \cos m\theta \int_0^{\infty} D_m^{(o)}(k,s) I_m(kq) \sin kx \, dk \right\} \quad \text{for } q < 1 \quad (36)$$

The potentials 33 and 34 may be substituted in the boundary conditions 3 and 5 to give

$$(\varphi_j' - \mu\varphi_o')_{q=1} = \epsilon_1 \left\{ (\sin \theta + h) \int_x^{x_s} [\xi^2 + s^2 + 1 - 2s \cos(\theta + \alpha)]^{-3/2} \, d\xi \right.$$

$$\left. - \frac{1}{s} hx [x^2 s^2 + s^2 + 1 - 2s \cos(\theta + \alpha)]^{-1/2} \right\} \quad (37)$$

$$\left(\frac{\partial \varphi_o'}{\partial q} - \mu \frac{\partial \varphi_j'}{\partial q} \right)_{q=1} = \mu\epsilon_1 \left\{ x(\sin \theta + h) [x^2 + s^2 + 1 - 2s \cos(\theta + \alpha)]^{-3/2} \right.$$

$$- hx[s - \cos(\theta + \alpha)] [x^2 s^2 + s^2 + 1 - 2s \cos(\theta + \alpha)]^{-3/2}$$

$$\left. - \frac{\partial}{\partial q} \int_x^{x_s} (q \sin \theta + hq^2) [\xi^2 + q^2 s^2 + 1 - 2sq \cos(\theta + \alpha)]^{-3/2} \, d\xi \right\}$$

$$(38)$$

in which $q = 1$ has to be substituted on the right-hand side. Integral representations of the F-functions similar to 22 have been used to obtain 37 and 38. The identities 25 - 29 are used to express 37 and 38 in the expanded form

$$(\varphi'_j - \mu\varphi'_o)_{q=1} = \frac{2\epsilon_1}{\pi} \int_0^\infty \sin kx \left\{ \sin \alpha \left[K_o(k)I_o(ks) - \frac{1}{s^2} K_1\left(\frac{k}{s}\right) I_o(k) \right] \right.$$

$$+ 2 \sum_{m=1}^\infty \left(\left[K_m(k)I'_m(ks) + \frac{1}{s^2} K'_m\left(\frac{k}{s}\right)I_m(k) \right] \sin \alpha \cos m(\alpha+\theta) \right.$$

$$\left. \left. + \frac{m}{ks} \left[K_m\left(\frac{k}{s}\right)I_m(k) - K_m(k)I_m(ks) \right] \cos \alpha \sin m(\alpha+\theta) \right) \right\} dk$$

$$(39)$$

$$\left(\frac{\partial \varphi'_o}{\partial q} - \frac{\partial \varphi'_j}{\partial q} \right)_{q=1} = \frac{2\mu\epsilon_1}{\pi} \int_0^\infty \sin kx \left\{ - k \sin \alpha \left[K_1(k)I_1(ks) - \frac{1}{s^2} K_1\left(\frac{k}{s}\right)I_1(k) \right] \right.$$

$$+ 2 \sum_{m=1}^\infty \left(k \left[K'_m(k)I'_m(ks) - \frac{1}{s^2} K'_m\left(\frac{k}{s}\right)I'_m(k) \right] \sin \alpha \cos m(\alpha+\theta) \right.$$

$$\left. \left. - \frac{m}{s} \left[K_m\left(\frac{k}{s}\right)I'_m(k) + K'_m(k)I_m(ks) \right] \cos \alpha \sin m(\alpha+\theta) \right) \right\} dk$$

$$(40)$$

The boundary conditions 39 and 40 are now used to determine the coefficients T_m and D_m of the expansions 35 and 36 for φ'_o and φ'_j as

$$T_m^{(o)}(k,s) = 2\epsilon_1(1-\epsilon_2)k \frac{I_m K_m' + K_m I_m'}{1-\epsilon_1 k(I_m K_m' + K_m I_m')} \left\{ \frac{m}{ks} I_m(ks)\cos\alpha\cos m\alpha \right.$$

$$\left. + I_m'(ks)\sin\alpha\sin m\alpha \right\} \tag{41a}$$

$$T_m^{(j)}(k,s) = 2\epsilon_1\left\{ \frac{m}{ks}\left[K_m(\frac{k}{s}) + \frac{2kK_m K_m' I_m(ks)}{1-\epsilon_1 k(I_m K_m' + K_m I_m')} \right]\cos\alpha\cos m\alpha \right.$$

$$\left. -\left[\frac{1}{s^2}K_m'(\frac{k}{s}) - \frac{2kK_m K_m' I_m'(ks)}{1-\epsilon_1 k(I_m K_m' + K_m I_m')}\right]\sin\alpha\sin m\alpha \right\} \tag{41b}$$

$$D_m^{(o)}(k,s) = 2\epsilon_1(1-\epsilon_2)k \frac{I_m K_m' + K_m I_m'}{1-\epsilon_1 k(I_m K_m' + K_m I_m')} \left\{ \frac{m}{ks} I_m(ks)\cos\alpha\sin m\alpha \right.$$

$$\left. - I_m'(ks)\sin\alpha\cos m\alpha \right\} \tag{41c}$$

$$D_m^{(j)}(k,s) = 2\epsilon_1\left\{ \frac{m}{ks}\left[K_m(\frac{k}{s}) + \frac{2kK_m K_m' I_m(ks)}{1-\epsilon_1 k(I_m K_m' + K_m I_m')} \right]\cos\alpha\sin m\alpha \right.$$

$$\left. +\left[\frac{1}{s^2}K_m'(\frac{k}{s}) - \frac{2kK_m K_m' I_m'(ks)}{1-\epsilon_1 k(I_m K_m' + K_m I_m')}\right]\sin\alpha\cos m\alpha \right\} \tag{41d}$$

The argument for the Bessel functions of argument k has been omitted. The three-dimensional part of the solution for the vortex element lying inside the jet may now be obtained from 33, 34, and 35, 36 together with equations 41.

E. SOLUTION FOR A LINE VORTEX DISTRIBUTION

The solutions obtained previously for an arbitrarily placed vortex element are now used to determine the solution for a vortex line of distribution $\Gamma(y)$. The vortex line lies along the line $x = 0$, $z = -h$, from $y = -b_2$ to $y = b_1$. The two- and three-dimensional parts of the solution are added together, using the relevant solution for the vortex distribution inside and outside the jet, to give for the perturbation velocity potential $\varphi(x, y, z)$

$$\varphi = \varphi_o \quad \text{for} \quad q > 1; \quad \varphi = \varphi_j \quad \text{for} \quad q < 1$$

where

$$4\pi\varphi_o = \int_{-b_1}^{b_2} \Gamma(\eta)F(x, y-\eta, z+h)d\eta \; - \; \epsilon_2\int_{-h'}^{h'}\Gamma(\eta)F(x, y-\eta, z+h)d\eta$$

$$+ \epsilon_1\left(\int_{-b_2}^{-h'} + \int_{h'}^{b_1}\right) \frac{1}{s^4}\Gamma(\eta)\left[(\eta^2-h^2)F(x, y-\frac{\eta}{s^2}, z+\frac{h}{s^2})\right.$$

$$\left. + 2\eta hG(x, y-\frac{\eta}{s^2}, z+\frac{h}{s^2})\right] d\eta$$

$$+ \frac{2}{\pi}\sum_{m=0}^{\infty}\int_0^{\infty}K_m(kq)\sin kx$$

$$\times \left\{\sin m\theta\left[\left(\int_{-b_2}^{-h'} + \int_{h'}^{b_1}\right)\Gamma(\eta)S_m^{(o)}(k, \eta)d\eta + \int_{-h'}^{h'}\Gamma(\eta)T_m^{(o)}(k, \eta)d\eta\right]\right.$$

$$\left. + \cos m\theta\left[\left(\int_{-b_2}^{-h'} + \int_{h'}^{b_1}\right)\Gamma(\eta)C_m^{(o)}(k, \eta)d\eta + \int_{-h'}^{h'}\Gamma(\eta)D_m^{(o)}(k, \eta)d\eta\right]\right\} dk$$

$$(42a)$$

$$4\pi\varphi_j = \int_{-b_1}^{b_2} \Gamma(\eta)F(x,y-\eta,z+h)d\eta - \epsilon_2\left(\int_{-b_2}^{-h'} + \int_{-h'}^{b_1}\right)\Gamma(\eta)F(x,y-\eta,z+h)\,d\eta$$

$$- \epsilon_1\int_{-h'}^{h'} \frac{1}{s^4}\Gamma(\eta)\left[(\eta^2-h^2)F(x,y-\frac{\eta}{s^2},z+\frac{h}{s^2})d\eta\right.$$

$$\left. + 2\eta h G(x,y-\frac{\eta}{s^2},z+\frac{h}{s^2})\right]\,d\eta$$

$$+ \frac{2}{\pi}\sum_{m=0}^{\infty}\int_0^{\infty} I_m(kq)\sin kx$$

$$\times \left\{\sin m\theta\left[\left(\int_{-b_2}^{-h'} + \int_{h'}^{b_1}\right)\Gamma(\eta)S_m^{(j)}(k,\eta)d\eta + \int_{-h'}^{h'}\Gamma(\eta)T_m^{(j)}(k,\eta)d\eta\right]\right.$$

$$\left. + \cos m\theta\left[\left(\int_{-b_2}^{-h'} + \int_{h'}^{b_1}\right)\Gamma(\eta)C_m^{(j)}(k,\eta)d\eta + \int_{-h'}^{h'}\Gamma(\eta)D_m^{(j)}(k,\eta)d\eta\right]\right\}\,dk$$

$$(42b)$$

In the above expressions, the functions F and G are given by

$$F(x,y,z) = F_1(y,z) + F_2(x,y,z) = \frac{z}{y^2+z^2}\left[1 + x(x^2+y^2+z^2)^{-1/2}\right] \quad (43a)$$

$$G(x,y,z) = F_3(y,z) + F_4(x,y,z) = \frac{y}{y^2+z^2}\left[1 + x(x^2+y^2+z^2)^{-1/2}\right] \quad (43b)$$

respectively.

III. SOLUTION FOR A WING AT A HIGH ANGLE OF ATTACK
IN A SINGLE JET

A. FORMULATION

A solution is presented here which determines the effect of a single jet slipstream on a wing held at an angle of attack which is not small. Angles of attack sufficient to cause separation of the flow are excluded. This section presents the solution for a single jet located centrally along the span of a wing whose planform is taken as rectangular and whose chord is untwisted. This solution will be extended in Section IV to the multiple jet case. Further extensions to cases of non-rectangular planform and small twist follow from the method used in this section but they are not investigated.

The Weissinger method is used to determine the flow over a wing at a moderate angle of incidence. In this method, the wing is divided chordwise into a number of sections. The flow past a particular section is approximated by a vortex line distribution along the quarter-chord line of the section. The solution for this flow is obtained from Section II, taking into account the position in the jet of the relevant section. The total solution is then the sum of the solutions over all the sections. The boundary condition of zero normal flow at the wing is then applied at the three-quarter chord point of each section and at a sufficient number of points along the three-quarter chord line to compute the assumed vorticity distributions to reasonable accuracy.

The wing is taken with its leading edge along the line $x = 0$, $z = l$, for $|y| < b$, and the chord line (from leading to trailing edge) at an angle α to the stream, e.g. see Fig. 2. The wing shape is taken to have the form

$$z' = S(x') \tag{44}$$

where the coordinates x', z' run from the leading edge along the chord to the trailing edge and perpendicular to it, respectively. The shape of the wing in the x, z coordinates is taken as

$$z = H(x) \tag{45}$$

where $H(x)$ is to be found from the equations

$$H(x) = \ell \ - \ x' \sin \alpha + S(x') \sin \alpha \ ,$$
$$x = x' \cos \alpha + S(x') \sin \alpha \tag{46}$$

The projection of the chord on the x-axis is given by

$$c_1 = c \cos \alpha \tag{47}$$

where c is the chord length of the wing.

The wing is divided into N sections. Let

$$d_N = \frac{c_1}{N} \tag{48}$$

A section is defined by the range

$$(n-1)d_N < x < nd_N \qquad \text{for} \ \ n = 1, 2, \ldots, N \tag{49}$$

A vortex line distribution is placed along the quarter-chord line of each section, that is, along the line given by

$$x = (n-1)d_N + \frac{1}{4}d_N = x_n, \quad \text{say,} \tag{50}$$

and

$$z = H(x_n) = -h_n, \quad \text{say} . \tag{51}$$

The boundary condition on the wing will be evaluated along the three-quarter

chord line of each section, that is, along the line given by

$$x = (n-1)d_N + \frac{3}{4} d_N = X_n, \text{ say,} \tag{52}$$

and

$$z = H(X_n) = H_n, \text{ say .} \tag{53}$$

The vortex line distribution at the quarter-chord line of the nth section is represented by $\Gamma(y) = \Gamma_n(y)$. The solution for this vortex distribution along the line $x = x_n$, $z = -h_n$, is obtained from the solution given in Section II-E by substituting $(x-x_n)$ for x, h_n for h, and $\Gamma_n(y)$ for $\Gamma(y)$. Call this solution $\varphi_n(x, y, z)$. Hence

$$\varphi_n = \varphi(x-x_n, y, z ; \quad \Gamma = \Gamma_n, \ h = h_n) \tag{54}$$

and the total solution, summing over all the sections of the wing, is given by

$$\Phi = \sum_{n=1}^{N} \varphi_n \tag{55}$$

B. FOURIER EXPANSION FOR THE CIRCULATION

For the case of a wing square in planform with a circular jet located along the mid-span, it is convenient to adopt the following notation (see Fig. 3). At the three-quarter chord line of each section of the wing the span is divided into two regions: $R_{o,n}$ outside the jet and $R_{1,n}$ inside the jet. That is,

$$R_{1,n}: \quad |y| < h_n' \quad \text{and} \quad R_{o,n}: \quad h_n' < |y| < b \tag{56}$$

where

$$h_n' = \sqrt{1 - h_n^2} \tag{57}$$

The angles $\psi_{o,n}$ and $\psi_{1,n}$ at each section are defined by

$$y = b \cos \psi_{o,n} \qquad \text{for} \quad h_n' < |y| < b \tag{58}$$

$$y = b \cos \psi_{o,n} = h_n' \cos \psi_{1,n} \qquad \text{for} \quad |y| < h_n' \tag{59}$$

The circulation functions $\Gamma_n(y)$ are expanded as Fourier series in terms of the angles $\psi_{o,n}$, $\psi_{1,n}$ in the regions $R_{o,n}$ and $R_{1,n}$. In deciding on the particular form of these functions, it is instructive to look at the local lift distributions. By the Joukowsky law, the lift at a section of the wing is given by

$$\ell_n(y) = \ell \, V_{local} \Gamma_n(y) \tag{60}$$

The lift distribution is continuous across the boundaries of the jet. Hence

$$\Gamma_n(h_n' - ih_n - 0) = \mu \Gamma_n(h_n' - ih_n + 0)$$

and $\tag{61}$

$$\Gamma_n(-h_n' - ih_n + 0) = \mu \Gamma_n(-h_n' - ih_n - 0)$$

From this it can be seen that the circulation function $\Gamma_n(y)$ has a discontinuity at the jet boundary. Also, in order to account for a small slipstream rotation, odd functions of y in Γ are allowed inside the jet. The proposed expansion for $\Gamma_n(y)$ is

$$\Gamma_n(y) = 4bV_j \begin{cases} \displaystyle\sum_{\lambda=1}^{2\Lambda} A_{\lambda,n}^{(o)} \sin \lambda \psi_{o,n} = \Gamma_{o,n} & \text{in } R_{o,n} \\[2em] \Gamma_{o,n} + A_{o,n}^{(1)} + B_{o,n}^{(1)} \cos \psi_{1,n} + \displaystyle\sum_{\lambda=1}^{2\Lambda'} A_{\lambda,n}^{(1)} \sin \lambda \psi_{o,n} = \Gamma_{1,n} & \text{in } R_{1,n} \end{cases} \tag{62}$$

in which Λ and Λ' may depend on n; that is, the number of terms taken in the expansions may vary with distance of the section downstream. The choice of Λ and Λ' will be determined by the accuracy required in the solution consistent with the computing procedure adopted. In 62 the terms $A_{o,n}^{(1)}$ and $B_{o,n}^{(1)} \cos \psi_{1,n}$ introduce a discontinuity in the circulation at the jet boundary. The slipstream rotation is represented by the term $B_{o,n}^{(1)} \cos \psi_{1,n}$ and the terms involving $A_{2\lambda,n}$.

Application of the conditions 61 of the continuity of lift at the jet boundaries gives

$$A_{o,n}^{(1)} = (\mu - 1) \sum_{\lambda=0}^{\Lambda-1} A_{2\lambda+1,n}^{(o)} \sin (2\lambda+1)\beta_n \tag{63}$$

$$B_{o,n}^{(1)} = (\mu - 1) \sum_{\lambda=0}^{\Lambda} A_{2\lambda,n}^{(o)} \sin 2\lambda\beta_n \tag{64}$$

where

$$\beta_n = \cos^{-1} \frac{h_n'}{b} \tag{65}$$

On neglect of slipstream rotation and with a wing symmetric about the mid-span, the circulation will be an even function about the mid-span which indicates $A_{2\lambda,n}^{(1)} = A_{2\lambda,n}^{(o)} = 0$ and hence $\beta_{o,n}^{(1)} = 0$.

The total lift on the wing is given by

$$L = \sum_{n=1}^{N} L_n \tag{66}$$

where L_n is the lift developed by each section of the wing. That is, using 60 and 62

$$L_n = 4\rho b V_j \left\{ \int_{R_o} V_o \Gamma_{o,n} dy + \int_{R_1} V_j \Gamma_{1,n} dy \right\} \qquad (67)$$

Substitution of the expansions 62 for $\Gamma_{o,n}$ and $\Gamma_{1,n}$ then yields

$$\frac{L_n}{8\rho b V_j^2} = h_n'(A_{o,n}^{(1)} + \frac{\pi}{4} A_{1,n}^{(1)}) + \frac{\pi}{4} b A_{1,n}^{(o)}$$

$$+ (\mu-1)b \sum_{\lambda=0}^{\Lambda-1} A_{2\lambda+1,n}^{(o)} \left\{ \frac{\sin 2\lambda\beta_n}{4\lambda} - \frac{\sin 2(\lambda+1)\beta_n}{4(\lambda+1)} \right\} \qquad (68)$$

C. DOWNWASH DISTRIBUTION

In order to apply the boundary condition of zero normal velocity at the wing, it is necessary to calculate the downwash. The boundary condition will be applied along the three-quarter chord line of each section of the wing, that is along $x = X_r$, $z = H_r$ (see 52 and 53). The downwash velocity at $x = X_r$ is defined as

$$w(y) = -\left[\frac{\partial \Phi}{\partial z} \right]_{x=X_r, z=H_r}$$

$$= -\left[\frac{\partial}{\partial z} \sum_{n=1}^{N} \varphi(X_r - x_n, y, z; \Gamma = \Gamma_n, h = h_n) \right]_{z=H_r} \qquad (69)$$

where φ is given in II-E. The downwash is split into its even and odd functions of y, which are denoted by

$$w(y) = \begin{cases} w_{o,ev} + w_{o,od} & \text{for } |y| > H_r' = \sqrt{1 - H_r^2} \\ \\ w_{j,ev} + w_{j,od} & \text{for } |y| < H_r' \end{cases} \qquad (70)$$

- 24 -

The subscripts o and j again denote the regions outside and inside the jet.

Using the expansion 62 for the circulation functions Γ_n in the expression 69, the downwash at $x = X_r$ may be evaluated in the following form:

$$
-4\pi(w_{o,ev} + w_{o,od}) = \sum_{n=1}^{N} \Bigg\{ {}_1N_n + {}_2N_n + {}_3N_n + \frac{2}{\pi} \int_0^\infty \sin k(X_r - x_n) \sum_{m=0}^{\infty}
$$

$$
\times \Bigg[\left(k \sin\theta \sin m\theta \, K_m'(kq) + \frac{m}{q} \cos\theta \cos m\theta \, K_m(kq) \right)
$$

$$
\times \left(\left[\int_{-b}^{-h_n'} + \int_{h_n'}^{b} \right] \Gamma_n(\eta) S_m^{(o)}(k,\eta) d\eta + \int_{-h_n'}^{h_n'} \Gamma_n(\eta) T_m^{(o)}(k,\eta) d\eta \right)
$$

$$
+ \left(k \sin\theta \cos m\theta \, K_m'(kq) - \frac{m}{q} \cos\theta \sin m\theta \, K_m(kq) \right)
$$

$$
\times \left(\left[\int_{-b}^{-h_n'} + \int_{-h_n'}^{b} \right] \Gamma_n(\eta) C_m^{(o)}(k,\eta) d\eta + \int_{-h_n'}^{h_n'} \Gamma_n(\eta) D_m^{(o)}(k,\eta) d\eta \right) \Bigg] dk \Bigg\}
$$

(71a)

$$
-4\pi(w_{j,ev} + w_{j,od}) = \sum_{n=1}^{N} \Bigg\{ {}_1N_n + {}_4N_n + {}_5N_n + \frac{2}{\pi} \int_0^\infty \sin k(X_r - x_n) \sum_{m=0}^{\infty}
$$

$$
\times \Bigg[\left(k \sin\theta \sin m\theta \, I_m'(kq) + \frac{m}{q} \cos\theta \cos m\theta \, I_m(kq) \right)
$$

$$
\times \left(\left[\int_{-b}^{-h_n'} + \int_{h_n'}^{b} \right] \Gamma_n(\eta) S_m^{(j)}(k,\eta) d\eta + \int_{-h_n'}^{h_n'} \Gamma_n(\eta) T_m^{(j)}(k,\eta) d\eta \right)
$$

$$
+ \left(k \sin\theta \cos m\theta \, I_m'(kq) - \frac{m}{q} \cos\theta \sin m\theta \, I_m(kq) \right)
$$

$$
\times \left(\left[\int_{-b}^{-h_n'} + \int_{h_n'}^{b} \right] \Gamma_n(\eta) C_m^{(j)}(k,\eta) d\eta + \int_{-h_n'}^{h_n'} \Gamma_n(\eta) D_m^{(j)}(k,\eta) d\eta \right) \Bigg] dk \Bigg\}
$$

(71b)

where $q^2 = y^2 + H_r^2$ and $\theta = \tan^{-1} \dfrac{H_r}{y}$ have to be substituted on the right-hand side. The N functions are defined by

$$
{}_1N_n = 4b^2 V_j \sum_{\lambda=1}^{2\Lambda} A_{\lambda,n}^{(o)} \left[{}_1I_o^\pi + {}_2I_o^\pi - {}_3I_o^\pi \right]
$$

$$
+ \, 4bh_n' V_j \Bigg(A_{o,n}^{(1)} \left[{}_4I + {}_5I - {}_6I \right] + B_{o,n}^{(1)} \left[{}_7I + {}_8I - {}_9I \right]
$$

$$
+ \sum_{\lambda=1}^{2\Lambda'} A_{\lambda,n}^{(1)} \left[{}_1I_o^\pi + {}_2I_o^\pi - {}_3I_o^\pi \right] \Bigg) \tag{72a}
$$

$$
{}_2N_n = -4b^2 V_j \epsilon_2 \sum_{\lambda=1}^{2\Lambda} A_{\lambda,n}^{(o)} \left[{}_1I_{\beta_n}^{\pi-\beta_n} + {}_2I_{\beta_n}^{\pi-\beta_n} - {}_3I_{\beta_n}^{\pi-\beta_n} \right]
$$

$$
- \, 4bh_n' V_j \epsilon_2 \Bigg(A_{o,n}^{(1)} \left[{}_4I + {}_5I - {}_6I \right] + B_{o,n}^{(1)} \left[{}_7I + {}_8I - {}_9I \right]
$$

$$
+ \sum_{\lambda=1}^{2\Lambda'} A_{\lambda,n}^{(1)} \left[{}_1I_o^\pi + {}_2I_o^\pi - {}_3I_o^\pi \right] \Bigg) \tag{72b}
$$

$$
{}_3N_n = 4b^2 V_j \epsilon_1 \sum_{\lambda=1}^{2\Lambda} A_{\lambda,n}^{(o)} \Big\{ {}_{10}I_o^{\beta_n} + {}_{10}I_{\pi-\beta_n}^\pi + {}_{11}I_o^{\beta_n} + {}_{11}I_{\pi-\beta_n}^\pi
$$

$$
- {}_{12}I_o^{\beta_n} - {}_{12}I_{\pi-\beta_n}^\pi - {}_{19}I_o^{\beta_n} - {}_{19}I_{\pi-\beta_n}^\pi \Big\} \tag{72c}
$$

$$
{}_4I_n = -4b^2 V_j \epsilon_2 \sum_{\lambda=1}^{2\Lambda} A_{\lambda,n}^{(o)} \Big\{ {}_1I_o^{\beta_n} + {}_1I_{\pi-\beta_n}^\pi + {}_2I_o^{\beta_n} + {}_2I_{\pi-\beta_n}^\pi - {}_3I_o^{\beta_n} - {}_3I_{\pi-\beta_n}^\pi \Big\} \tag{72d}
$$

$$5^I{}_n = -4b^2 V_j \epsilon_1 \sum_{\lambda=1}^{2\Lambda} A_{\lambda,n}^{(o)} [{}_{10}I_{\beta_n}^{\pi-\beta_n} + {}_{11}I_{\beta_n}^{\pi-\beta_n} - {}_{12}I_{\beta_n}^{\pi-\beta_n} - {}_{19}I_{\beta_n}^{\pi-\beta_n}]$$

$$- 4bh'_n V_j \epsilon_1 \left(A_{o,n}^{(1)} [{}_{13}I + {}_{14}I - {}_{15}I - {}_{20}I] + B_{o,n}^{(1)} [{}_{16}I + {}_{17}I - {}_{18}I - {}_{21}I] \right.$$

$$\left. + \sum_{\lambda=1}^{2\Lambda'} A_{\lambda,n}^{(1)} [{}_{10}I_o^{\pi} + {}_{11}I_o^{\pi} - {}_{12}I_o^{\pi} - {}_{19}I_o^{\pi}] \right) \tag{72e}$$

In the above expressions a dash on a Bessel function denotes differentiation with respect to the argument. The I functions are defined in Appendix I. The even and odd parts in the N functions are determined by taking λ odd and even, respectively, in the series terms together with the terms containing $A_{o,n}^{(1)}$ in the even part and $B_{o,n}^{(1)}$ in the odd part. The remaining terms on the right-hand sides of 72 may be split into their even and odd parts by taking the even part to contain only odd values of m in the series containing S_m and T_m and even values of m in the series containing C_m and D_m. The odd part is then given by the remaining terms in these series.

D. BOUNDARY CONDITIONS ON THE WING

A slipstream rotation is considered which has the following properties. The slipstream may have a rotational velocity component about its own axis. The angular velocity is denoted by $\omega(q)$, where q is the radial distance from the axis; ω is taken positive if the rotation is counterclockwise when viewed from the rear. It is assumed that $|\omega|_{max} << V_j$. The slipstream rotation is assumed to have no effect outside the jet. Its effect inside the jet is a change in the fluid direction at the wing, resulting in an effective variation of

wing incidence. A variation of the angular velocity $\omega(q)$ in the downstream direction may be included using the analysis presented here, but this will not be done.

The local geometric angle of attack of the wing along the three-quarter chord line of the rth section of the wing is denoted by $\alpha_r(y)$. It is assumed that the geometric wing incidence is symmetric in y, i. e. that $\alpha_r(y) = \alpha_r(-y)$. The boundary condition of the tangency of the fluid velocity at the wing gives

$$w(X_r, y) = V_o \alpha_r(y) \qquad \text{for } |y| > H_r' \qquad (73a)$$

$$w(X_r, y) - \sqrt{y^2 + H_r^2}\, \omega(\sqrt{y^2 + H_r^2})\sin \frac{y}{H_r} = V_j \alpha_r(y) \quad \text{for } |y| < H_r' \quad (73b)$$

along the three-quarter chord line of each section of the wing, that is, for $r = 1, \ldots, N$. The positive square root is taken in 73b. The definition 70, splitting the downwash w into its even and odd components inside and outside the jet, may be used to achieve a similar splitting of 73 as

$$w_{o, ev}(X_r, y) = V_o \alpha_r(y) \qquad \text{for } H_r' < y < b \qquad (74a)$$

$$w_{o, od}(X_r, y) = 0 \qquad \text{for } H_r' < y < b \qquad (74b)$$

$$w_{j, ev}(X_r, y) = V_j \alpha_r(y) \qquad \text{for } 0 < y < H_r' \qquad (74c)$$

$$w_{j, od}(X_r, y) = \sqrt{y^2 + H_r^2}\, \omega(\sqrt{y^2 + H_r^2})\sin \frac{y}{H_r} \quad \text{for } 0 < y < H_r'$$

$$(74d)$$

Equations 71 and 74 provide a system of linear algebraic equations for the determination of the coefficients $A_{\lambda,n}^{(o)}$, $A_{\lambda,n}^{(1)}$, $A_{o,n}^{(1)}$, $B_{o,n}^{(1)}$ in the Fourier expansion 62 of the circulation. The boundary condition represented by 74 must be applied at sufficiently many points y along the wing to obtain a determinable system of equations for these coefficients. If an equal number of coefficients is used at each section, the number of equations involved will be N times that of the single section wing used in the example treated by Wu. A feature of the present work, however, is that the singularities present in the Wu solution (where the boundary condition is applied on $z = 0$) do not appear. This is due to the presence of terms of the type $(H_r + h_n)^2$ in the denominator of the integrals in the Appendix; these terms never vanish and prevent a singularity in the integral. Under these circumstances the constrains on the coefficients sufficient to exclude such singularities, as adopted by Wu, are relaxed here. The boundary condition 74 must be applied at a compensating number of points y along the wing to make up the equations released by the relaxed constraints.

IV. EXTENSION TO MULTIPLE JETS

A. NOMENCLATURE

A system of $2J$ jet slipstreams, symmetrically placed with respect to the mid span, is considered. The wing span is divided into $(2J+1)$ regions, denoted by R_ν, $\nu = 0, 1, \ldots, 2J$ which are defined as follows: R_0 is the region outboard of all the jets, $R_{2\nu-1}$ is the region inside the νth jet pair, $\nu = 1, 2, \ldots, J$, counted from the wing tip toward the center, $R_{2\nu}$ is the region between the νth and the $(\nu+1)^{th}$ jet pairs. The width of these regions will vary in the downstream direction according to the inclination of the wing. The boundaries of the regions along the y-axis are given by the points

$$b_o = b, b_1, b_2, \ldots, b_{2J}, b_{2J+1}, = 0, \qquad b_{-2J}, \ldots, -b_1, -b_o = -b \; .$$

The center of the νth jet is along the line defined by $z = 0$ and

$$y = \pm a_\nu \; , \quad a_\nu = \frac{1}{2}(b_{2\nu-1} + b_{2\nu})$$

The wing will be taken to have a square planform and to have no span-wise twist. At a station x downstream, therefore, the wing will be a distance h below the center-line of the jets. The intersections of the wing with the boundary of the νth jet at the station x is given by $z = -h$ and $y = a_\nu \pm h'$, where $h' = \sqrt{1-h^2}$, which we denoted by $y = c_{2\nu-1}$ and $y = c_{2\nu}$, respectively. Hence a point y in the region R_ν may be found from

$$y = c_s \cos \psi_s \; , \quad s = 0, 1, \ldots, \nu \tag{75}$$

At the point $y = c_\nu$

$$\psi_s = \beta_s^{(\nu)} = \cos^{-1}\left(\frac{c_\nu}{c_s}\right) \qquad s = 0, 1, \ldots, \nu \tag{76}$$
$$\nu = 0, 1, \ldots, 2J$$

- 30 -

Fig. 4 gives a guide to the nomenclature defined above.

B. FOURIER EXPANSION FOR THE CIRCULATION

The Weissinger approximation will be used to determine the circulation distribution over the wing. The lift is given by

$$L = \sum_{n=1}^{N} \int_{span} \ell_n(y)dy = \rho \sum_{n=1}^{N} \int_{span} V_{local} \Gamma_n(y)dy$$

where Γ_n is the circulation distribution at each section of the wing. The lift distribution is continuous at the boundaries of the jet. Hence at the points $z = -h, \ y = c_1, c_2, \ldots, c_{2J}$

$$\Gamma_{n,\, 2\nu-1}(c_{2\nu-1}-ih-0) = \mu\Gamma_{n,\, 2\nu-2}(c_{2\nu-1}-ih+0)$$

$$\Gamma_{n,\, 2\nu-1}(c_{2\nu}-ih+0) = \mu\Gamma_{n,\, 2\nu}(c_{2\nu}-ih-0)$$

(77)

where the second subscript on Γ denotes the region in which Γ is defined.

The circulation distribution $\Gamma_n(y)$ at each section is defined in each region R_ν, for $\nu = 0, 1, \ldots, 2J$, by

$$\Gamma_n(y) = 4bV_j\Gamma_{n,\, \nu}(y)$$

(78)

where

$$\Gamma_{n,\, o}(y) = \sum_{\lambda=0}^{\Lambda_o-1} A_{2\lambda+1,\, n}^{(o)} \sin(2\lambda+1)\psi_{o,\, n}$$

$$\Gamma_{n,\, \nu}(y) = \Gamma_{n,\nu-1}(y) + A_{n,\, o}^{(\nu)} + \sum_{\lambda=0}^{\Lambda_\nu-1} A_{2\lambda+1,\, n}^{(\nu)} \sin(2\lambda+1)\psi_{\nu,\, n}$$

Here the dependence of the angles ψ on the wing section chosen has been noted. The region R_ν is also dependent on n, being defined by $c_{\nu,n} \geq y \geq c_{\nu+1,n}$ where $c_{\nu,n} = a_\nu - \sqrt{1 - h_n^2}$. An alternative writing of 78 is

$$\Gamma_{n,\nu}(y) = \sum_{s=0}^{\nu} \left\{ A_{o,n}^{(s)} + \sum_{\lambda=0}^{\Lambda_s - 1} A_{2\lambda+1,n}^{(s)} \sin(2\lambda+1)\psi_{s,n} \right\} \quad \text{for } \nu = 0,1,\ldots, 2J \tag{79}$$

with

$$A_{o,n}^{(o)} = 0$$

Only odd multiples of the angles ψ are taken in 78, which relies on the assumption that the geometric incidence of the wing and the rotation of the slipstream be symmetric about the mid-span.

The boundary conditions 77 may be used to express the coefficients $A_{o,n}^{(\nu)}$ in terms of the unknown coefficients $A_{2\lambda+1,n}^{(s)}$ in the form

$$A_{o,n}^{(\nu)} = \left\{ \begin{matrix} (\mu-1) \\ (\frac{1}{\mu}-1) \end{matrix} \right\} \sum_{s=0}^{\nu-1} \left[A_{o,n}^{(s)} + \sum_{\lambda=0}^{\Lambda_s-1} A_{2\lambda+1,n}^{(s)} \sin(2\lambda+1)\beta_{s,n}^{(\nu)} \right] \text{for} \left\{ \begin{matrix} \nu = 1,3,\ldots, 2J-1 \\ \nu = 2,4,\ldots, 2J \end{matrix} \right\} \tag{80}$$

The total lift may now be evaluated as

$$\frac{L}{8\rho b V_j^2} = \sum_{n=1}^{N} \left\{ \sum_{\nu=0}^{2J} c_{\nu,n} \left[A_{o,n}^{(\nu)} + \frac{\pi}{4} A_{1,n}^{(\nu)} \right] + (\mu-1) \sum_{\nu=0}^{J} \sum_{s=0}^{2\nu} \left[(c_{2\nu,n} - c_{2\nu-1,n}) A_{o,n}^{(s)} \right. \right.$$
$$+ c_{\nu,n} \sum_{\lambda=0}^{\Lambda_s-1} A_{2\lambda+1,n}^{(s)} \left(\frac{\sin 2\lambda\beta_{s,n}^{(2\nu+1)} - \sin 2\lambda\beta_{s,n}^{(2\nu)}}{4\lambda} \right.$$
$$\left. \left. \left. - \frac{\sin 2(\lambda+1)\beta_{s,n}^{(2\nu+1)} - \sin 2(\lambda+1)\beta_{s,n}^{(2\nu)}}{4(\lambda+1)} \right) \right] \right\}$$

- 32 -

C. VELOCITY POTENTIAL

The velocity potential of a vortex element at an arbitrary height with respect to a single jet slipstream has been determined in Section II. The method used there involved the construction of the image system of the vortex element in the jet. The two-dimensional part of the solution was found directly this way. A similar image system was used in the three-dimensional part of the solution, leaving a remainder term which was evaluated analytically. The velocity potential due to a vortex element placed in a system of multiple jets will be constructed using this image method as follows. The vortex element has images due to each jet separately. Each image then has further images due to the rest of the jets. An image system of infinite order is thereby generated. An approximate solution is presented which takes into account the primary image system and the first order corrections due to these images, i. e. the image-image contributions. However, only the primary image system is used in the remainder term of the three-dimensional part of the solution. It is anticipated that this term is already small and the first order corrections are neglected.

The two-dimensional part of the velocity potential, denoting the potential outside all the jets by φ_0 and the potential inside the λth jet by $\varphi_{j,\lambda}$, is made up from the following contributions. The factor $\frac{1}{4\pi}\Gamma(\eta)d\eta$ is omitted.

(I) For a vortex element $\Gamma(\eta)d\eta$ located at $y = \eta$, $z = -h$, taken outside the jets

$$
\varphi_0 \left\{ \begin{array}{l} F_1(y-\eta, z+h) \text{ plus a sum over } \nu \text{ of the image in each jet, i. e.} \\[2mm] \dfrac{\epsilon_1}{[(\eta-a_\nu)^2+h^2]^2}\left[((\eta-a_\nu)^2-h^2)F_1\left(y-a_\nu - \dfrac{\eta-a_\nu}{(\eta-a_\nu)^2+h^2}, z + \dfrac{h}{(\eta-a_\nu)^2+h^2}\right)\right. \\[4mm] \left. \hspace{2cm} + 2(\eta-a_\nu)hF_3(\text{same argument as } F_1) \right] \end{array}\right.
$$

This latter function will be denoted by χ_ν.

$$\varphi_{j,\lambda} \begin{cases} (1-\epsilon_2)F_1(y-\eta, z+h) \text{ plus the images of this image due to the other jets,} \\ \text{i. e. a sum over all } \nu \neq \lambda \text{ of } (1-\epsilon_2)\,\chi_\nu. \end{cases}$$

(II) For the vortex inside the ℓth jet, $\ell \neq \lambda$

$$\varphi_o \begin{cases} (1-\epsilon_2)F_1(y-\eta, z-h) \text{ plus this image reflected in the other jets, i. e. a} \\ \text{sum over all } \nu \neq \ell \quad \text{of } (1-\epsilon_2)\,\chi_\nu \end{cases}$$

$$\varphi_{j,\lambda \neq \ell} \begin{cases} (1-\epsilon_2)^2 F_1(y-\eta, z+h) \end{cases}$$

(III) For the vortex inside the λth jet

$$\varphi_o \begin{cases} \text{same system as (II)} \end{cases}$$

$$\varphi_{j,\lambda} \begin{cases} F_1(y-\eta, z+h) \text{ and the single image } -\chi_\lambda. \text{ The vortex element reflected} \\ \text{in all the other jets gives the contribution } (1-\epsilon_2)^2 \chi_\nu \text{ summed over} \\ \text{all } \nu \neq \lambda. \end{cases}$$

The construction of an image system to represent part of the three-dimensional component of the solution is accomplished as above for the two-dimensional part; the remainder term is approximated by the primary image system only. The complete velocity potential may now be written down. Using the substitutions

$$y-a_\nu = r_\nu \cos\theta_\nu \qquad\qquad z = r_\nu \sin\theta_\nu$$

$$y + a_\nu = r_{-\nu} \cos\theta_{-\nu} \qquad\qquad z = r_{-\nu} \sin\theta_{-\nu} \,,$$

and the symmetry about the mid-span, the velocity potential, φ_o, outside the

jets is given by

$$4\pi\varphi_o = \int_{-b}^{b} \Gamma(\eta)F(x, y-\eta, z+h)d\eta - \epsilon_2 \sum_{\ell=1}^{J} \int_{c_{2\ell}}^{c_{2\ell-1}} \Gamma(\eta)\left[F(x, y-\eta, z+h)+F(x, y+\eta, z+h)\right]d\eta$$

$$+ \int_{-b}^{b} \Gamma(\eta)\left\{\sum_{\nu=1}^{J}\left[x'(\eta,a_\nu) + x'(-\eta,-a_\nu)\right]\right\}d\eta$$

$$- (1-\epsilon_2)\sum_{\ell=1}^{J} \int_{c_{2\ell}}^{c_{2\ell-1}} \Gamma(\eta)\left[x'(\eta,a_\ell) + x'(-\eta,a_\ell)\right]d\eta$$

$$- \epsilon_2 \sum_{\ell=1}^{J}\sum_{\nu=1}^{J} \int_{c_{2\ell}}^{c_{2\ell-1}} \Gamma(\eta)\left[x'(\eta,a_\nu) + x'(-\eta,-a_\nu) + x'(-\eta,a_\nu) + x'(\eta,-a_\nu)\right]d\eta$$

$$+ \frac{2}{\pi}\sum_{\ell=1}^{J}\sum_{m=0}^{\infty}\int_{0}^{\infty}\sin kx$$

$$\times \sin m\theta_\ell\, K_m(kq_\ell)\left[\left(\int_{c_{2\ell+1}}^{c_{2\ell}} + \int_{c_{2\ell-1}}^{c_{2\ell-2}}\right)\Gamma(\eta)S_m^{(o)}(k,\eta)d\eta\right.$$

$$\left. + \int_{c_{2\ell}}^{c_{2\ell-1}} \Gamma(\eta)T_m^{(o)}(k,\eta)d\eta\right]$$

$$+ \cos m\theta_\ell\, K_m(kq_\ell)\left[\left(\int_{c_{2\ell+1}}^{c_{2\ell}} + \int_{c_{2\ell-1}}^{c_{2\ell-2}}\right)\Gamma(\eta)C_m^{(o)}(k,\eta)d\eta\right.$$

$$\left. + \int_{c_{2\ell}}^{c_{2\ell-1}} \Gamma(\eta)D_m^{(o)}(k,\eta)d\eta\right]$$

$$+ \sin m\theta_{-\ell} K_m(kq_\ell)\left[\left(\int_{c_{-2\ell+2}}^{c_{-2\ell+1}} + \int_{c_{-2\ell}}^{c_{-2\ell-1}}\right)\Gamma(\eta)S_m^{(o)}(k,\eta)d\eta\right.$$

$$+ \int_{c_{-2\ell+1}}^{c_{-2\ell}} \Gamma(\eta) T_m^{(o)}(k, \eta) d\eta \Bigg]$$

$$+ \cos m\theta_{-\ell} K_m(kq_{-\ell}) \left[\left(\int_{c_{-2\ell+2}}^{c_{-2\ell+1}} + \int_{c_{-2\ell}}^{c_{-2\ell-1}} \right) \Gamma(\eta) C_m^{(o)}(k, \eta) d\eta \right.$$

$$\left. + \int_{c_{-2\ell+1}}^{c_{-2\ell}} \Gamma(\eta) D_m^{(o)}(k, \eta) d\eta \right] \Bigg\} dk$$

where $x'(\eta, a_\nu)$ is the extension to three-dimensions of the function χ_ν used above, that is

$$x'(\eta, a_\nu) = \frac{\epsilon_1}{[(\eta - a_\nu)^2 + h^2]^2} \left[\left((\eta - a_\nu)^2 - h^2 \right) F\left(x, y - a_\nu - \frac{\eta - a_\nu}{(\eta - a_\nu)^2 + h^2}, z + \frac{h}{(\eta - a_\nu)^2 + h^2} \right) \right.$$

$$\left. + 2(\eta - a_\nu) hG(\text{same argument as } F) \right]$$

The velocity potential, $\varphi_{j,\lambda}$, inside the λth jet is given by

$$4\pi \varphi_{j,\lambda} = (1 - \epsilon_2) \int_{-b}^{b} \Gamma(\eta) F(x, y - \eta, z + h) d\eta$$

$$- \epsilon_2 (1 - \epsilon_2) \sum_{\ell=1}^{J} \int_{c_{2\ell}}^{c_{2\ell-1}} \Gamma(\eta) \left[F(x, y - \eta, z + h) + F(x, y + \eta, z + h) \right] d\eta$$

$$+ (1 - \epsilon_2) \sum_{\ell=1}^{J} \int_{c_{2\ell+1}}^{c_{2\ell}} \Gamma(\eta) \left[\sum_{\nu=1}^{J} \left\{ x'(\eta, a_\nu) + x'(\eta, -a_\nu) + x'(-\eta, a_\nu) + x'(-\eta, -a_\nu) \right\} \right.$$

$$\left. - x'(\eta, a_\lambda) - x'(-\eta, a_\lambda) \right] d\eta$$

$$+ \int_{c_{2\lambda}}^{c_{2\lambda-1}} \Gamma(\eta) \left[F(x, y-\eta, z+h) - (1-\epsilon_2)^2 \left[F(x, y-\eta, z+h) + F(x, y+\eta, z+h) \right] \right.$$

$$\left. + (1-\epsilon_2)^2 \left\{ \sum_{\nu=1}^{J} \left[\chi'(\eta, a_\nu) + \chi'(\eta, -a_\nu) \right] - \chi'(\eta, a_\lambda) \right\} \right] d\eta$$

$$+ \frac{2}{\pi} \sum_{\ell=1}^{J} \sum_{m=0}^{\infty} \int_{0}^{\infty} \sin kx$$

$$\times \sin m\theta_\ell I_m(kq_\ell) \left[\left(\int_{c_{2\ell+1}}^{c_{2\ell}} + \int_{c_{2\ell-1}}^{c_{2\ell-2}} \right) \Gamma(\eta) S_m^{(j)}(k,\eta) d\eta \right.$$

$$\left. + \int_{c_{2\ell}}^{c_{2\ell-1}} \Gamma(\eta) T_m^{(j)}(k,\eta) d\eta \right]$$

$$+ \cos m\theta_\ell I_m(kq_\ell) \left[\left(\int_{c_{2\ell+1}}^{c_{2\ell}} + \int_{c_{2\ell-1}}^{c_{2\ell-2}} \right) \Gamma(\eta) C_m^{(j)}(k,\eta) d\eta \right.$$

$$\left. + \int_{c_{2\ell}}^{c_{2\ell-1}} \Gamma(\eta) D_m^{(j)}(k,\eta) d\eta \right]$$

$$+ \sin m\theta_{-\ell} I_m(kq_{-\ell}) \left[\left(\int_{c_{-2\ell+2}}^{c_{-2\ell+1}} + \int_{c_{-2\ell}}^{c_{2\ell-1}} \right) \Gamma(\eta) S_m^{(j)}(k,\eta) d\eta \right.$$

$$\left. + \int_{c_{-2\ell+1}}^{c_{2\ell}} \Gamma(\eta) T_m^{(j)}(k,\eta) d\eta \right]$$

$$+ \cos m\theta_{-\ell} I_m(kq_{-\ell}) \left[\left(\int_{c_{-2\ell+2}}^{c_{-2\ell+1}} + \int_{c_{-2\ell}}^{c_{2\ell-1}} \right) \Gamma(\eta) C_m^{(j)}(k,\eta) d\eta \right.$$

$$\left. \left. + \int_{c_{-2\ell+1}}^{c_{-2\ell}} \Gamma(\eta) D_m^{(j)}(k,\eta) d\eta \right] \right\} dk$$

D. DOWNWASH AND BOUNDARY CONDITIONS

The downwash distribution corresponding to the velocity potential for the multiple jet case obtained in the previous section may be obtained in similar fashion to the simple jet case (see 71). The integrals involved will be those listed in the Appendix. It is not intended to write down the downwash here as it is a complicated expression. Assumption of a slipstream rotation of the type described in III-D will lead to similar boundary conditions to 73 in each region R_ν (see also Wu), and the determination of the coefficients in the expansion 79 for the circulation will proceed as before from the solution of a system of linear equations.

V. CONCLUSIONS AND RECOMMENDATIONS

Prediction of the spanwise lift distribution on a wing at an arbitrary height and high angle of attack extending through multiple jets (propeller slipstreams) has been accomplished by the present theory.

Implementation of the theory requires both an extensive machine programming effort and experimental confirmation. The mathematical complexity encountered in the theory requires close coordination between the analytical and machine programming efforts.

It is therefore recommended that the following two (2) steps be undertaken:

1. Extensive machine calculations - a programming effort directed towards systematically developing a generalized calculation program employing the wing and slipstream geometry as inputs should be undertaken. This program should then be used to calculate spanwise lift distributions of a broad spectrum of arrangements to (1) delineate significant trends due to non-uniform flow effects and (2) provide results for comparison with experimental data.

2. Systematic Experimental Program - wind tunnel tests to confirm the analytical results and determine real fluid effects should be conducted. The tests should be designed to yield accurate spanwise lift distributions of wing-slipstream arrangements selected from the analytical study above to yield a meaningful confirmation of the theory.

APPENDIX

A series of integral functions denoted by $_kI_\alpha^\beta$ were introduced in Section III-C. These integrals will be defined in the following and the parameters used in their definitions will be noted as arguments. A number of supplementary functions are used which are given by

$$A(\theta) = \frac{(y - b\cos\theta)^2 - (H_r + h_n)^2}{[(y - b\cos\theta)^2 + (H_r + h_n)^2]^2} \sin\theta$$

$$B(\theta) = [(y - b\cos\theta)^2 + (H_r + h_n)^2]^{-1} \sin\theta$$

$$C(\theta) = [(X_r - x_n)^2 + (y - b\cos\theta)^2 + (H_r + h_n)^2]^{-1/2}$$

$$D_1(\theta) = \frac{b^2\cos^2\theta - h_n^2}{[b^2\cos^2\theta + h_n^2]^2} \sin\theta$$

$$D_2(\theta) = \frac{2bh_n\sin\theta\cos\theta}{(b^2\cos^2\theta + h_n^2)^2} \left(y - \frac{b\cos\theta}{b^2\cos^2\theta + h_n^2}\right)\left(H_r + \frac{h_n}{b^2\cos^2\theta + h_n^2}\right)$$

$$E_1(\theta) = \left(y - \frac{b\cos\theta}{b^2\cos^2\theta + h_n^2}\right)^2 - \left(H_r + \frac{h_n}{b^2\cos^2\theta + h_n^2}\right)^2$$

$$E_2(\theta) = \left[\left(y - \frac{b\cos\theta}{b^2\cos^2\theta + h_n^2}\right)^2 + \left(H_r + \frac{h_n}{b^2\cos^2\theta + h_n^2}\right)^2\right]^{-1}$$

$$L(\theta) = [(X_r - x_n)^2 + E_2^{-1}(\theta)]^{-1/2}$$

$$M(\theta) = \left(H_r + \frac{h_n}{b^2\cos^2\theta + h_n^2}\right)^2$$

The integrals $_nI_\alpha^\beta$ are defined by

$$_1I_\alpha^\beta (y, b, H_r, h_n, \lambda) = \int_\alpha^\beta A(\theta) \sin \lambda\theta \, d\theta$$

$$_2I_\alpha^\beta (y, b, H_r, h_n, X_r, x_n, \lambda) = (X_r - x_n)\int_\alpha^\beta A(\theta)C(\theta) \sin \lambda\theta \, d\theta$$

$$_3I_\alpha^\beta (y, b, H_r, h_n, X_r, x_n, \lambda) = (X_r - x_n)(H_r + h_n)^2\int_\alpha^\beta B(\theta)C^3(\theta) \sin \lambda\theta \, d\theta$$

$$_4I (y, b, H_r, h_n) = \int_0^\pi A(\theta)d\theta$$

$$_5I (y, b, H_r, h_n, X_r, x_n) = (X_r - x_n)\int_0^\pi A(\theta)C(\theta)d\theta$$

$$_6I (y, b, H_r, h_n, X_r, x_n) = (X_r - x_n)(H_r + h_n)^2 \int_0^\pi B(\theta)C^3(\theta) \, d\theta$$

$$_7I (y, b, H_r, h_n) = \int_0^\pi A(\theta) \cos \theta \, d\theta$$

$$_8I (y, b, H_r, h_n, X_r, x_n) = (X_r - x_n)\int_0^\pi A(\theta)C(\theta) \cos \theta \, d\theta$$

$$_9I (y, b, H_r, h_n, X_r, x_n) = (X_r - x_n)(H_r + h_n)^2 \int_0^\pi B(\theta)C^3(\theta) \cos \theta \, d\theta$$

$$_{10}I_\alpha^\beta (y, b, H_r, h_n, \lambda) = \int_\alpha^\beta D_1(\theta)E_1(\theta)E_2^2(\theta) \sin \lambda\theta \, d\theta$$

$$_{11}I_\alpha^\beta (y, b, H_r, h_n, X_r, x_n, \lambda) = (X_r - x_n)\int_\alpha^\beta D_1(\theta)E_1(\theta)E_2^2(\theta)L(\theta) \sin \lambda\theta \, d\theta$$

$$_{12}I_\alpha^\beta (y, b, H_r, h_n, X_r, x_n, \lambda) = (X_r - x_n)\int_\alpha^\beta D_1(\theta)E_2(\theta)L^3(\theta)M(\theta) \sin \lambda\theta \, d\theta$$

$$_{13}I(y,b,H_r,h_n) = \int_0^\pi D_1(\theta)E_1(\theta)E_2^2(\theta)\,d\theta$$

$$_{14}I(y,b,H_r,h_n,X_r,x_n) = (X_r-x_n)\int_0^\pi D_1(\theta)E_1(\theta)E_2^2(\theta)L(\theta)\,d\theta$$

$$_{15}I(y,b,H_r,h_n,X_r,x_n) = (X_r-x_n)\int_0^\pi D_1(\theta)E_2(\theta)L^3(\theta)M(\theta)\,d\theta$$

$$_{16}I(y,b,H_r,h_n) = \int_0^\pi D_1(\theta)E_1(\theta)E_2^2(\theta)L(\theta)\cos\theta\,d\theta$$

$$_{17}I(y,b,H_r,h_n,X_r,x_n) = (X_r-x_n)\int_0^\pi D_1(\theta)E_1(\theta)E_2^2(\theta)L(\theta)\cos\theta\,d\theta$$

$$_{18}I(y,b,H_r,h_n,X_r,x_n) = (X_r-x_n)\int_0^\pi D_1(\theta)E_2(\theta)L^3(\theta)M(\theta)\cos\theta\,d\theta$$

$$_{19}I_\alpha^\beta(y,b,H_r,h_n,X_r,x_n,\lambda) = \int_\alpha^\beta D_2(\theta)E_2^2(\theta)\,[\,2+3(X_r-x_n)L(\theta)$$

$$-(X_r-x_n)^3L^3(\theta)]\sin\lambda\theta\,d\theta$$

$$_{20}I(y,b,H_r,h_n,X_r,x_n) = \int_0^\pi D_2(\theta)E_2^2(\theta)\,[\,2+3(X_r-x_n)L(\theta)-(X_r-x_n)^3L^3(\theta)]\,d\theta$$

$$_{21}I(y\ b,H_r,h_n,X_r,x_n) = \int_0^\pi D_2(\theta)E_2^2(\theta)\,[\,2+3(X_r-x_n)L(\theta)$$

$$-(X_r-x_n)^3L^3(\theta)]\cos\theta\,d\theta$$

REFERENCES

1. Wu, T. Y. and Talmadge, Richard B. : A Lifting Surface Theory for Wings Extending Through Multiple Jets. Vehicle Research Corporation Report No. 8, 1961.

2. Rethorst, S. : Aerodynamics of Non-uniform Flows as Related to an Airfoil Extending Through a Circular Jet. J. Aero. Sci., Vol. 25, No. 1, pp. 11-28, 1958

3. Rethorst, S. ; Royce, W. W. ; and Wu, T. Y. : Lift Characteristics of Wings Extending Through Propeller Slipstreams. Vehicle Research Corporation Report No. 1, 1958

4. Watson, G. N. : Bessel Functions. Cambridge University Press, London, 1948
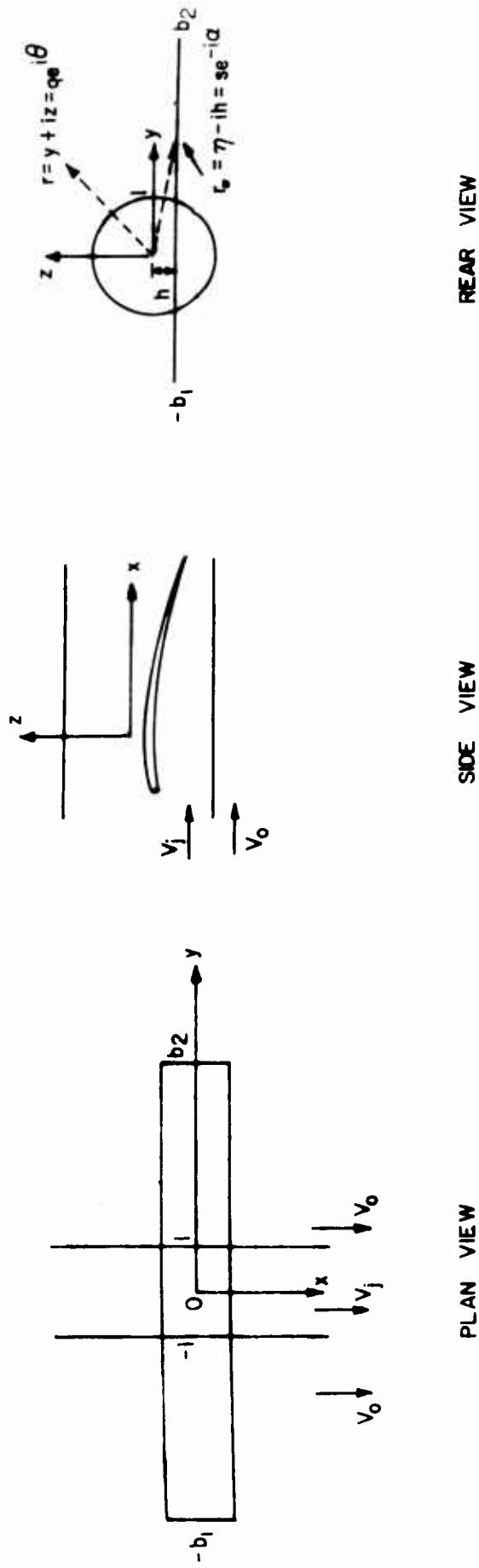
SINGLE JET PASSING OVER WING OF SMALL CHORD ASSUMED

LOCATED A DISTANCE h BELOW CENTER LINE OF JET

FIG. 1

WING SHAPE
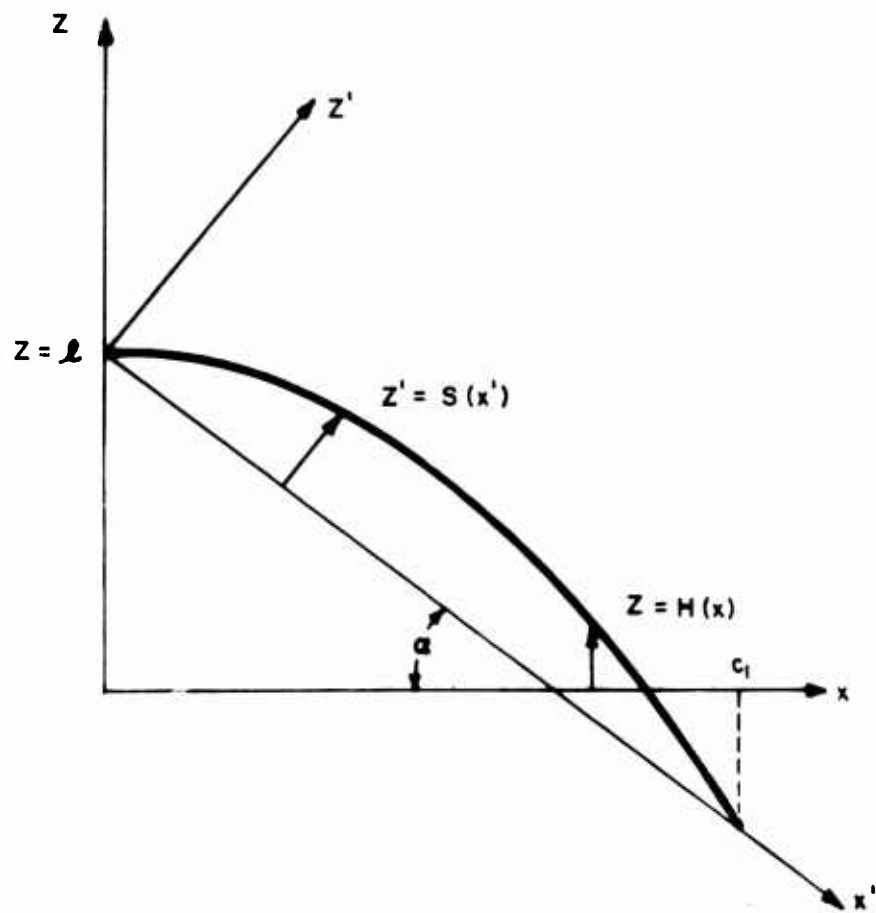
FIG. 2

DIAGRAM INDICATING NOTATION USED FOR A CIRCULATION JET
LOCATED ALONG MID-SPAN OF A SQUARE WING
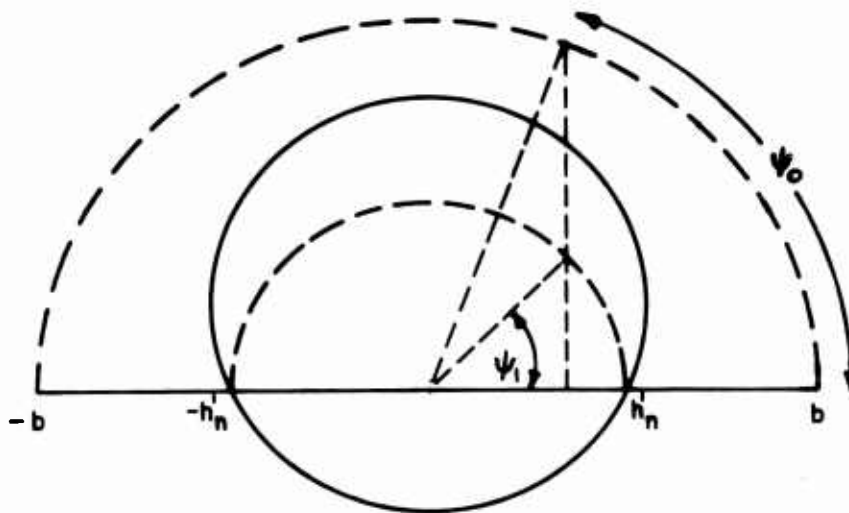
FIG. 3

MULTIPLE JET CONFIGURATION
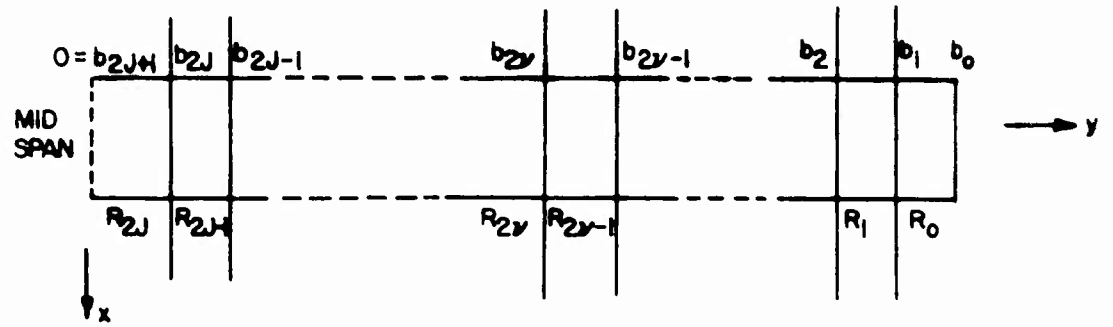
PLAN VIEW

(a)
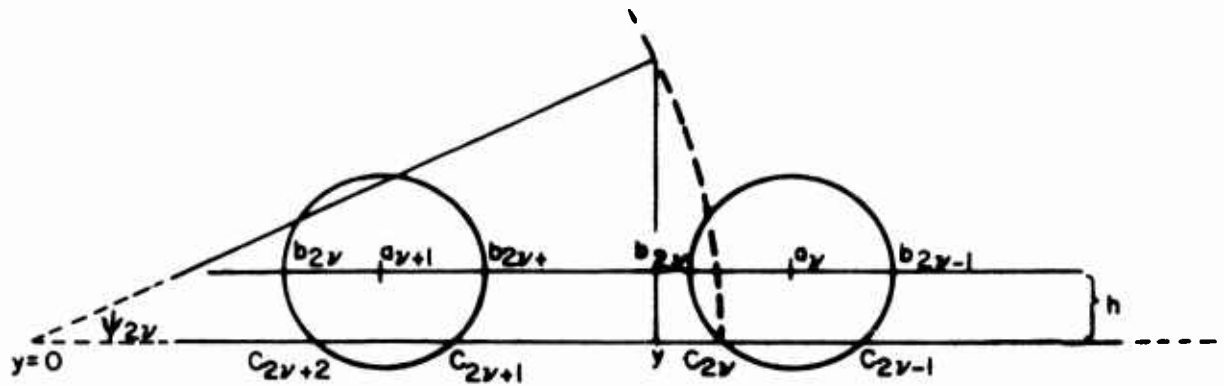
REAR VIEW

(b)

FIG. 4

DISTRIBUTION LIST

Chief, Bureau of Naval Weapons
(RAAD-3)
Department of the Navy
Washington 25, D.C.

Chief, Bureau of Naval Weapons
(RA-4)
Department of the Navy
Washington 25, D.C.

Chief, Bureau of Naval Weapons
(RR-25)
Department of the Navy
Washington 25, D.C.

Chief, Bureau of Naval Weapons
(RR-55)
Department of the Navy
Washington 25, D.C.

Commanding Officer and Director
David Taylor Model Basin
Aerodynamics Laboratory
Washington 7, D.C.

Chief of Naval Operations (OP-07T)
Department of the Navy
Washington 25, D.C.

Chief of Naval Research (Code 461)
Department of the Navy
Washington 25, D.C.
(4 copies)

Commanding Officer
Office of Naval Research Branch Office
Navy #100, Box #39, F.P.O.
New York, New York
ATTN: Head, Documents Section
(2 copies)

Commanding Officer
Office of Naval Research Branch Office
346 Broadway
New York 13, New York

Commanding Officer
Office of Naval Research Branch Office
The John Crerar Library Building
86 E. Randolph Street
Chicago 1, Illinois

Commanding Officer
Office of Naval Research Branch Office
1030 E. Green Street
Pasadena, California

Director
Naval Research Laboratory
Technical Information Office
Washington 25, D.C.
(6 copies)

Commandant of the Marine Corps
Code AAP
Arlington Annex
Washington 25, D.C.

Marine Corps Development Center
Marine Corps School
Quantico, Virginia
ATTN: Air Section

U. S. Air Force (SRGL)
Office of Scientific Research
Washington 25, D.C.

Wright Air Development Division
Directorate of Systems Management
(WWZT)
Wright-Patterson A.F.B., Ohio

Wright Air Development Division
Advanced Systems Technology (WWRPS)
Wright-Patterson A.F.B., Ohio

Office of Chief of Transportation
(TAFO-R)
Department of the Army
Washington 25, D.C.
(2 copies)

Agricultural & Mechanical College
of Texas
Aeronautical Engineering Department
College Station, Texas
ATTN: Prof. F. Weick

University of Washington
Department of Aeronautical Engineering
Seattle 5, Washington
ATTN: Prof. F.S. Eastman

University of Wichita
Department of Engineering Research
Wichita 14, Kansas
ATTN: Dean K. Razak

Aerophysics Corporation
17 Dupont Circle
Washington 6, D.C.
ATTN: Dr. G. Boehler

Armour Research Foundation
3440 South State Street
Chicago, Illinois

AVCO Manufacturing Corporation
Lycoming Division
550 South Main Street
Stratford, Connecticut
ATTN: Dr. Fritz Haber

Beech Aircraft Corporation
Wichita, Kansas
ATTN: Mr. M.J. Gordon

Bell Aerosystems Company
P. O. Box 1
Buffalo 5, New York
ATTN: Advanced Design

Bell Helicopter Corporation
P.O. Box No. 482
Fort Worth 1, Texas
ATTN: Mr. B. Kelly, V.P.
Engineering

Boeing Airplane Company
Wichita, Kansas
ATTN: Mr. H. Higgens

Cessna Aircraft Company
Wallace Plant
Wichita, Kansas

Collins Radio Company
Cedar Rapids, Iowa
ATTN: Dr. A. Lippisch

Convair Division
General Dynamics Corporation
Fort Worth, Texas
ATTN: Chief Engineer

Convair Division
General Dynamics Corporation
Pomona, California

Cornell Aeronautical Laboratory, Inc.
4455 Genesee Street
Buffalo 21, New York
ATTN: Mr. H.A. Cheilek

Douglas Aircraft Company, Inc.
El Segundo Division
El Segundo, California
ATTN: Chief Engineer

Fairchild Aircraft & Missiles Division
Research Department
Hagerstown, Maryland
ATTN: Mr. R. Darby

Goodyear Aircraft Corporation
1210 Massillon Road
Akron 15, Ohio
ATTN: Dr. R. Ross

Cornell University
Graduate School of Aeronautics
Ithaca, New York
ATTN: Dr. W.R. Sears

Georgia Institute of Technology
Guggenheim School of Aeronautics
Atlanta, Georgia
ATTN: Dr. W. Dutton
      W. Castles

The Johns Hopkins University
Applied Physics Laboratory
Baltimore 18, Maryland
ATTN: Dr. F.H. Clauser
      Mr. D.W. Rabenhorst

The Johns Hopkins University
Mechanical Engineering Department
Baltimore 18, Maryland
ATTN: Dr. Stanley Corrsin

Massachusetts Institute of Technology
Aeronautical Engineering Department
Cambridge 30, Massachusetts
ATTN: Dr. R.H. Miller

Mississippi State University
Engineering and Industrial Research
                          Station
State College, Mississippi
ATTN: Aerophysics Department

Naval Postgraduate School
Aeronautical Engineering Department
Monterey, California
ATTN: Dr. R. Head

University of Michigan
Department of Aeronautical Engineering
Ann Arbor, Michigan
ATTN: Dr. W. Nelson

University of Minnesota
Aeronautical Engineering Department
Minneapolis 14, Minnesota
ATTN: Prof. J.A. Akerman

New York University
Aeronautical Engineering Department
New York, New York
ATTN: Dr. Lee Arnold

Technological Institute
Northwestern University
Mechanical Engineering Department
Evanston, Illinois
ATTN: Prof. A.B. Cambel

Ohio State University
Department of Aeronautical Engineering
Columbus 10, Ohio
ATTN: Prof. G.L. vonEschen

Princeton University
Aeronautical Engineering Department
James Forrestal Research Center
Princeton, New Jersey
ATTN: Prof. D.C. Hazen
       Prof. A.A. Nikolsky

Purdue University
Aeronautical Engineering Department
Lafayette, Indiana

Rensselaer Polytechnic Institute
Aeronautical Engineering Department
Troy, New York

Stanford University
Guggenheim School of Aeronautics
Stanford, California
ATTN: Prof. E.G. Reid

Stevens Institute of Technology
Fluid Dynamics Laboratory
Hoboken, New Jersey
ATTN: Mr. L.H. Mott

Syracuse University
Mechanical Engineering Department
Syracuse, New York
ATTN: Dr. S. Eskinasi

Grumman Aircraft Engineering Corp.
Bethpage, L.I., New York
ATTN: Dr. C.E. Mack, Chief, Research
        Mr. F. T. Kurt

Hiller Aircraft Corporation
Advanced Research Division
1350 Willow Road
Palo Alto, California
ATTN: Dr. J. Sissingh

Hughes Tool Company
Aircraft Division
Culver City, California
ATTN: Chief Engineer

Kaman Aircraft Corporation
Old Windsor Road
Bloomfield, Connecticut
ATTN: Mr. J. Thomas

Lockheed Aircraft Corporation
Georgia Division
86 S. Cobb Drive
Marietta, Georgia

The Martin Company
Baltimore 3, Maryland
ATTN: Chief Engineer

McDonnell Aircraft Corporation
St. Louis, Missouri
ATTN: Chief Engineer

North American Aviation, Inc.
Columbus Division
Columbus 16, Ohio

Northrup Aircraft, Inc.
Hawthorne, California
ATTN: Dr. W. Pfenninger

Piasecki Aircraft Corporation
Island Road, International Airport
Philadelphia 42, Pennsylvania
ATTN: Chief Engineer

Republic Aviation Corporation
Farmingdale, L.I., New York
ATTN: Chief Engineer

Ryan Aeronautical Company
Lindbergh Field
San Diego, California
ATTN: Chief Engineer

Therm, Inc.
Ithaca, New York
ATTN: Dr. Ritter

United Aircraft Corporation
Hamilton Standard Division
Windsor Locks, Connecticut
ATTN: Mr. G. Rosen

Pratt & Whitney Division
United Aircraft Corporation
400 Main Street
East Hartford, Connecticut

Vehicle Research Corporation
1661 Lombardy Road
Pasadena, California
ATTN: Dr. Scott Rethorst

Vertol Division, Boeing Airplane Co.
Woodland Avenue
Morton, Pennsylvania
ATTN: Mr. L.L. Douglas

VEHICLE RESEARCH CORPORATION, REPORT NO. 9
A LIFTING SURFACE THEORY FOR WINGS AT
HIGH ANGLES OF ATTACK. E. Cumberbatch
July 1963.

A lifting surface theory has been developed for wings located at arbitrary heights and high angles of attack (up to the inception of flow separation) in a stream containing an arbitrary number of multiple jets (propeller slipstream). This theory extends and generalizes the formulation of T. Y. Wu and Richard Talmadge (VRC Report No. 8) which was based on the original Rethorst Lifting Surface Solution.

The present theory was developed by first analyzing the simpler single jet case and then extending the analysis to encompass multiple jets. Thus, the analysis is systematically presented in the following order:

1. Wing at an Arbitrary Height in a Single Jet - a method similar to that employed in VRC Report No. 8 for the wing located along the axis of the jet was used to extend the solution to a wing located at any height in the jet.

2. Wing at a High Angel of Attack in a Single Jet - the lifting surface method of Weissinger was applied to chordwise wing sections each of which is treated in accordance with its height in the jet as determined in the previous step.

3. Wing at Arbitrary Height and High Angle of Attack Extending through Multiple Jets - the above single jet analyses were extended to the case of a wing immersed in a stream containing an arbitrary number of jets. The jets were located symmetrically in the spanwise direction.

The above generalized theory encompasses a broad spectrum of V/STOL aircraft. The prediction of wing-slipstream interactions afforded by the present analysis permits optimization of such V/STOL aircraft.

1. Incompressible Flow (1.1.1)
2. Wing Theory (1.2.2.1)
3. Propeller Slipstreams (1.5.4)
4. Aircraft Performance (1.7.1.3)
I. Cumberbatch, E.
II. Vehicle Research Corporation Report No. 9

VEHICLE RESEARCH CORPORATION, REPORT NO. 9
A LIFTING SURFACE THEORY FOR WINGS AT
HIGH ANGLES OF ATTACK. E. Cumberbatch
July 1963.

A lifting surface theory has been developed for wings located at arbitrary heights and high angles of attack (up to the inception of flow separation) in a stream containing an arbitrary number of multiple jets (propeller slipstream). This theory extends and generalizes the formulation of T. Y. Wu and Richard Talmadge (VRC Report No. 8) which was based on the original Rethorst Lifting Surface Solution.

The present theory was developed by first analyzing the simpler single jet case and then extending the analysis to encompass multiple jets. Thus, the analysis is systematically presented in the following order:

1. Wing at an Arbitrary Height in a Single Jet - a method similar to that employed in VRC Report No. 8 for the wing located along the axis of the jet was used to extend the solution to a wing located at any height in the jet.

2. Wing at a High Angle of Attack in a Single Jet - the lifting surface method of Weissinger was applied to chordwise wing sections each of which is treated in accordance with its height in the jet as determined in the previous step.

3. Wing at Arbitrary Height and High Angle of Attack Extending through Multiple Jets - the above single jet analyses were extended to the case of a wing immersed in a stream containing an arbitrary number of jets. The jets were located symmetrically in the spanwise direction.

The above generalized theory encompasses a broad spectrum of V/STOL aircraft. The prediction of wing-slipstream interactions afforded by the present analysis permits optimization of such V/STOL aircraft.

1. Incompressible Flow (1.1.1)
2. Wing Theory (1.2.2.1)
3. Propeller Slipstreams (1.5.4)
4. Aircraft Performance (1.7.1.3)
I. Cumberbatch, E.
II. Vehicle Research Corporation Report No. 9

UNCLASSIFIED